AD_____

Award Number: DAMD17-03-1-0004

TITLE: Oral Administration of N-acetyl-D Glucosamine Polymer Particles Down-Regulates Airway Allergic Responses

PRINCIPAL INVESTIGATOR: Yoshimi Shibata, Ph.D.

CONTRACTING ORGANIZATION: Florida Atlantic University
Boca Raton, FL 33431-0991

REPORT DATE: May 2008

TYPE OF REPORT: Annual

PREPARED FOR: U.S. Army Medical Research and Materiel Command
Fort Detrick, Maryland 21702-5012

REPORT DOCUMENTATION PAGE

Form Approved
OMB No. 0704-0188

1. REPORT DATE	2. REPORT TYPE	3. DATES COVERED
01-05-2008	Annual	24 Feb 2007– 23 Apr 2008

4. TITLE AND SUBTITLE

Oral Administration of N-acetyl-D Glucosamine Polymer Particles Down-Regulates Airway Allergic Responses

5a. CONTRACT NUMBER

5b. GRANT NUMBER
DAMD17-03-1-0004

5c. PROGRAM ELEMENT NUMBER

6. AUTHOR(S)

Yoshimi Shibata, Ph.D.

Email: yshibata@fau.edu

5d. PROJECT NUMBER

5e. TASK NUMBER

5f. WORK UNIT NUMBER

7. PERFORMING ORGANIZATION NAME(S) AND ADDRESS(ES)

Florida Atlantic University
Boca Raton, FL 33431-0991

8. PERFORMING ORGANIZATION REPORT NUMBER

9. SPONSORING / MONITORING AGENCY NAME(S) AND ADDRESS(ES)
U.S. Army Medical Research and Materiel Command
Fort Detrick, Maryland 21702-5012

10. SPONSOR/MONITOR'S ACRONYM(S)

11. SPONSOR/MONITOR'S REPORT NUMBER(S)

12. DISTRIBUTION / AVAILABILITY STATEMENT
Approved for Public Release; Distribution Unlimited

13. SUPPLEMENTARY NOTES

14. ABSTRACT
This is an annual report of the 5th grant year. PI and 2 Research Associates moved to the current Institute in 2003 from East Carolina University. The project was re-started in December 2004 with approval of no-cost extension until 5/23/2009. In this grant period, we established a method producing chitin particles at 10 – 100 gram per batch. Biological activities to induce IL-12 and TNFα in vitro and to down-regulate allergic responses in mice were tested and the product was qualified for the purpose. We are continued to establish a method for larger scale of production at 500 – 1,000 gram per batch. We also realized that several experiments in 2006 – 2007 might not be reliable due to some mice that were later found being infected with Helicobacter spp. These experiments will be re-examined.

15. SUBJECT TERMS
Childhood asthma, N-acetyl-D-glucosamine polymer, IL-12, GATA-3, T-bet, macrophages, airway hyperreactivity

16. SECURITY CLASSIFICATION OF:			17. LIMITATION OF ABSTRACT	18. NUMBER OF PAGES	19a. NAME OF RESPONSIBLE PERSON
a. REPORT	b. ABSTRACT	c. THIS PAGE			USAMRMC
U	U	U	UU	55	19b. TELEPHONE NUMBER *(include area code)*

Table of Contents

INTRODUCTION:
This annual report includes a brief summary of the year of 2007 – 2008 research and related activities supported by DAMD17-03-1-0004.

This project funded by DOD DAMD17-03-1-0004 was initiated at East Carolina University on February 24, 2003. PI and two research associates moved to the current institute, Florida Atlantic University (FAU), on September 30, 2003. The transfer of grantee institute was approved on December 1, 2004. Since then, the project has re-started with no-cost extension until May 23, 2009. Two postdoctoral research associates, Shoutaro Tsuji, Ph.D. and Makiko Y. Tsuji, DVM, Ph.D. joined the laboratory and conducted this project starting in April 2005 until December 2006. Tsutomu Shinohara, M.D., Ph.D., a pulmonary physician/scientist, has joined in May 2006 and conducted the project until March 2008.

BODY:
Task 1: To determine if oral administration of 1 – 4 μm particles of chitin will down-regulate airway hyperreactivity (AHR) and GATA-3 levels as a measure of Th2 responses, and enhance T-bet levels as a measure of Th1 responses in the lungs of mice that are sensitized with ragweed allergens.
a. Establish the effects of dose response of chitin particles (Months 1 – 4).
b. Establish therapeutic/prophylactic effects of chitin (Months 4 – 9).
c. Determine duration of chitin treatments (Months 8 - 12).

This has been completed.

Task 2: To determine if the effects of 1 – 4 μm particles of chitin on endogenous IL-12- or IFNγ- mediated down-regulation of airway allergic responses will be greater than those of HK-BCG, ODN-CpG or an equal number of particles of 1 – 10 μm chitin.

a. Establish comparative studies on the effects of 1 – 4 μm chitin, 1 – 10 μm chitin, HK-BCG and ODN-CpG (Months 12 - 24).

b. Study if endogenous IL-12 or IFNγ is required for the chitin-induced down-regulation of GATA-3-mediated allergic responses (Months 24 – 40).

We are still under evaluation whether our previous animal studies are valid, since some mice during the experiments (2006 – 2007) were later realized to be infected with *Helicobacter spp*.

This is because our additional studies indicated below demonstrated that pulmonary inflammation induced by microbes appears to be persistent in a microbe-dependent manner. We found that alveolar macrophages (M∅) are important to regulate persistent pulmonary inflammation in response to bioactive particles including HK-BCG, chitin particles and probably *Helicobacter*. Persistent pulmonary inflammation potentially influences to asthma development. An example of our study using HK-BCG is shown below.

Rationale: Induced cyclooxygenase-2 (COX-2) in tissue macrophages (M∅) increases prostaglandin E_2 (PGE_2) release, down-regulating granulomatous inflammation. In response to mycobacteira, local M∅ seem to express catalytically active or inactive COX-2. Perhaps, alveolar M∅ would express inactive COX-2 and release no PGE_2, to maintain persistent mycobacterial pulmonary inflammation.
Objective: To evaluate forms of catalytically active and inactive COX-2 in alveolar M∅ during the development of mycobacterial pulmonary inflammation.
Methods: Whole lungs of C57Bl/6 mice were lavaged with saline following i.n. administration of heat-killed *Mycobacterium bovis* BCG (HK-BCG). COX-2 expression and PGE_2 release by alveolar M∅ and concentrations of tumor necrosis factor (TNF)-α and nitric oxide in the lavage fluid were monitored.
Measurements and Main Results: Normal alveolar M∅ showed undetectable levels COX-2 by Western blot. However, 1d after administration, almost all alveolar M∅ phagocytosed HK-BCG and expressed significant

levels of catalytically inactive COX-2 and no increase of PGE_2 release. In contrast to mice given i.p. BCG where peritoneal M∅ containing BCG disappeared within 7 days, 28 days after intranasal administration, 68% of alveolar M∅ still contained BCG together with inactive form of COX-2. There was no alveolar M∅ with active form of COX-2. Significantly more TNF-α and nitrite levels in the lung lavage fluid were detected by 28 d compared to those in control fluid.
Conclusions: Our results indicate that inactive COX-2 and the lack of PGE_2 production by alveolar M∅ are associated with persist pulmonary inflammation caused by mycobacteria.

Task 3: To determine if M∅ will phagocytose more particles and produce more IL-12 in response to 1 – 4 μm chitin compared to 1 – 10 μm chitin.

a. Determine if M∅ treated with 1 – 4 μm chitin particles phagocytose more particles than when treated with an equivalent number of 1 – 10 μm chitin particles (Months 41 – 44).

b. Determine if 1 – 4 μm chitin particles induce more production of IL-12 than an equivalent number of 1 – 10 μm chitin particles (Months 45 – 48).

We found an important molecular mechanism that chitin microparticles induce beneficial Th1 adjuvant effects. A manuscript presenting this finding is under revision in the American Journal Physiology Cell Physiol. A copy of manuscript is attached in the Appendix Material. A summary of finding is shown below.

When macrophages phagocytose chitin microparticles, MAPK are immediately activated in a manner dependent on phagosome formation, followed by the release of Th1 cytokines, but not IL-10. To determine whether phagocytosis and macrophage activation in response to chitin microparticles are dependent on membrane cholesterol, RAW264.7 macrophages were treated with methyl-β-cytodextrin (MBCD) to remove membrane cholesterol and stimulated with chitin and bacterial components including two heat-killed (HK) *Mycobacterium bovis* BCG and an oligodeoxynucleotide of bacterial DNA (CpG-ODN) as comparison controls. The treatment did not alter chitin binding or the phagocytosis of chitin particles 20 min after stimulation. At the same time, however, chitin-induced phosphorylation of cellular MAPK was accelerated and enhanced in an MBCD dose dependent manner. The increased phosphorylation was also observed for chitin phagosome-associated p38 and ERK1/2. In contrast, CpG-ODN or HK-BCG induced activation of MAPK in MBCD-treated cells at levels comparable to, or only slightly more than, those of control cells. We also found that MBCD treatment enhanced the production of TNF-α and the expression of cyclooxygenase 2 (COX-2) in response to chitin microparticles. In neither MBCD- nor saline- treated macrophages, did chitin particles induce detectable IL-10 mRNA synthesis. CpG-ODN-induced MAPK phosphorylation, TNF-α production, and COX-2 expression were less sensitive to MBCD treatment. Among the inanimate particles studied, our results indicate that macrophage activation by chitin microparticles was most sensitive to cholesterol depletion, suggesting that membrane structures integrated by cholesterol are important for physiologic regulation of chitin microparticle-induced cellular activation.

KEY RESEARCH ACCOMPLISHMENTS:

#1-4 previous grant years.

#5-6 this grant period

1. Establishment of cellular mechanisms underlying phagocytosis of chitin particles and production of anti-inflammatory cytokines by macrophages.
2. Establishment of the chitin Th1 adjuvant which inhibits IL-10, a Th2 cytokine, production.
3. Finding a novel mechanism underlying chitin particles down-regulating the activities of COX-2 in a post-translational regulation.
4. Establishment of characterization of splenic PGE_2-releasing macrophages which induce a Th1-to-Th2 shift of immune responses.
5. Establishment of a method producing chitin particles up to 100 gram per batch and further development to establish to produce 500 – 1,000 gram per batch.
6. Finding a mechanism of alveolar macrophages leading persistent pulmonary inflammation in response to certain microbes.

REPORTABLE OUTCOMES:

Paper Published (2003 – 2007)

Van Scott MR, JL Hooker, D Ehrmann, Y Shibata, C Kukoly, K Salleng, G Westergaard, A Sandrasagra, J Nyce. Dust mite-induced asthma in Cynomolgus monkeys. *J Appl Physiol 96:1433-1444, 2003. Task 2.*

Shibata Y, A Nishiyama, H Ohata, J Gabbard, QN Myrvik, RA Henriksen. Differential effects of IL-10 on prostaglandin H synthase-2 expression and prostaglandin E_2 biosynthesis between spleen and bone marrow macrophages. *J. Leuko. Biol. 77:544-551, 2005.* Tasks 2 and 3.

Shibata Y, Henriksen RA, Honda I, Nakamura RM, Myrvik QN. Splenic PGE2-releasing macrophages regulate Th1 and Th2 immune responses in mice treated with heat-killed BCG. *J Leukoc Biol 78, 1281-1290, 2005.* Task 2.

Shibata Y. Radiosensitive macrophages and immune responses --- Prostaglandin E_2-releasing macrophages induce a Th1-to-Th2 shift of immune responses in chronic inflammation ---*Proceeding of "International Symposium on Low-Dose Radiation Exposures and Bio-Defense System.* Page 5, 2006. Task 2.

Shibata Y, J Gabbard, M Yamashita, S Tsuji, M Smith, A Nishiyama, RA Henriksen, QN Myrvik. Heat-killed BCG induces biphasic cyclooxygenase-2^+ splenic macrophage formation --- role of IL-10 and bone marrow precursors. *J Leukocyte Biol 80:590-598, 2006.* Task 2.

Nishiyama, A, S Tsuji, M Yamashita, RA Henriksen, QN Myrvik, Y Shibata. Phagocytosis of *N*-acetyl-D-glucosamine particles, a Th1 adjuvant, results in MAPK activation and TNF-α, but not IL-10, production. *Cell Immunol 239:103 – 112, 2006.* Tasks 1 and 3.

Shibata Y, H Ohata, M Yamashita, S Tsuji, JF Bradfield, RA Hendrickson, A Nishiyama, QN Myrvik. Immunologic response enhances atherosclerosis -- Th1-to-Th2 shift and calcified atherosclerosis in BCG-treated apolipoprotein $E^{-/-}$ mice. *Translational Research 149:62-69, 2007.* Task 2.

Yamashita M, A Nishiyama, QN Myrvik, RA Henriksen, S Tsuji, Y Shibata. Differential subcellular localization of COX-2 by macrophages phagocytosing *Mycobacterium bovis* BCG in vivo. *Am J Physiol (Cell Physiology) 293:C184-C190, 2007. Task 2.*

Tsuji S, M Yamashita, A Nishiyama, T Shinohara, Z. Li, QN Myrvik, DR Hoffman, RA Henriksen, Y Shibata. Differential structure and activity between human and mouse intelectin-1: human intelectin-1 is a disulfide-linked trimer, whereas mouse homologue is a monomer. *Glycobiology 17:1045-1051, 2007*. Task 2.

Yamashita M, T Shinohara, S Tsuji, QN Myrvik, A Nishiyama, RA Henriksen, Y Shibata. Catatlycially inactive cyclooxygenase 2 (COX-2) and absence of PGE2 biosynthesis in murine peritoneal macrophages following in vivo phagocytosis of heat-killed *Mycobacterium bovis* BCG. *J. Immunol.179:7072-7078, 2007*. Task 2.

Manuscript in press (2007-2008)

Nishiyama A, T Shinohara, S Tsuji, M Yamashita,RA Henriksen, QN Myrvik, **Y Shibata**. Depletion of cellular cholesterol enhances macrophage MAPK activation by chitin microparticles but not by heat-killed *Mycobacterium bovis* BCG. ***Am J Physiol Cell Physiol*** *(in revision).* Tasks 1 and 3.

Manuscript submitted or in preparation (2007 – 2008)

Shibata, Y, P Vos, QN Myrvik. Neutrophils from BCG-immunized mice enhance innate immunity against lethal challenges of *Listeria monocytogenes*. Submitted for publication. Task 2.

Shinohara T, M Yamashita, T Pantuso, S Shinohara, QN Myrvik, RA Henriksen and Y Shibata. Mechanisms of mycobacterial pulmonary inflammation --- persistent activation of alveolar macrophages expressing inactive cyclooxygenase-2 without PGE_2 biosynthesis. Submitted for publication. Task 2.

Presentations (2007- 2008)

Shinohara T, M Yamashita, A Nishiyama, S Tsuji, QN Myrvik, RA Henriksen , Y Shibata. Differential regulation of cyclooxygenase (COX) isoforms in alveolar and peritoneal macrophages from heat-killed *Mycobacterium bovis* BCG treated mice. Abstract was presented at AAI Meeting at Miami in May 2007.

Shibata Y, T Shinohara, S Tsuji, RA Henriksen, A Nishiyama, QN Myrvik, RA, M Yamashita. Catalytically inactive cyclooxygenase 2 (COX-2) and absence of PGE_2 biosynthesis in murine peritoneal macrophages following *in vivo* phagocytosis of heat-killed *Mycobacterium bovis* BCG. Abstract was presented at AAI Meeting at Miami in May 2007.

Shibata Y. COX-2^+ macrophages in chronic inflammation. Tokushima University Medical School, Japan, January 2008. .

Shibata Y. Heterogeneity of COX-2^+ activated macrophages induced by Mycobacterium bovis BCG. Florida International University, Miami, FL in February 2008.

US Patent (2007-2008)

US Patent File, "Chitin micro-particles as an adjuvant" by Yoshimi Shibata and Quentin N. Myrvik, 6/16/07, U.S. Application No. 11/763,941

EMPLOYMENT (2003 – 2008):

Postdoctoral Research Associates, who worked for the project were Hiroyoshi Ohata, May 2003 – October 2004, Akihito Nishiyama, Ph.D., May 2003 - January 2007, Shoutaro Tsuji, Ph.D. and Makiko Y. Tsuji, DVM, Ph.D., both April 2004 – December 2005, and Tsutomu Shinohara, M.D., Ph.D., May 2005 – March 2008. A Ph.D. graduate student, Traci Pantuso, has been working for the project since August 2007. Mari Kogiso, Ph.D. plans to join April 2008 to work for the project.

CONCLUSIONS:

The neonates and young children are more susceptible than the young to infections and frequently develop asthmatic problems (1, 2). The mechanism by which these populations become immunocompromised appears to be an altered regulation of immunity and not simple immune deficiency. It is likely that macrophages in these immunocompromised populations become hypofunctional with excessive production of PGE_2 and IL-10,

both of which enhance allergic Th2 responses. Our studies clearly demonstrated that administration of chitin particles resulted in blocking the production of IL-10 and COX-2/PGE_2biosynthesis, enhancing relative Th1 responses. In sharp contrast, bacterial Th1 adjuvants (heat-killed *Mycobacteirum bovis* BCG, CpG-ODN) enhances both IL-10 production and PGE_2 release in vitro (3-5). Thus chitin may be the most potent Th1 adjuvant presently available and is an attractive immunomodulator for allergic asthma. We also demonstrate that HK-BCG provides distinctive effects between in vitro and in vivo studies (6, 7). Further studies to understand the adjuvant effects of chitin microparticles are needed.

A composition and method for the preparation of micro-particles of chitin (a naturally occurring polymer of N-acetyl-D-glucosamine), the characterization of chitin micro-particles as an immune adjuvant and the use of chitin micro-particles to enhance protective immunity against intracellular infectious agents and diseases as well as to inhibit allergic responses and diseases. We have established a method to produce bioactive chitin micro-particles at scales of 100 gram. To perform Phase I clinical trials, a large scale of production line at 500 – 1,000 gram levels is needed. We plan to establish the scale-up method in collaboration with Yaizu Suisankagaku Industry Co. Ltd (YSK), Shizuoka, Japan, leading similar chitin products.

REFERENCES:

1. van Benten, I. J., C. M. van Drunen, L. P. Koopman, B. C. van Middelkoop, W. C. Hop, A. D. Osterhaus, H. J. Neijens, and W. J. Fokkens. 2005. Age- and infection-related maturation of the nasal immune response in 0-2-year-old children. *Allergy* 60:226-232.
2. Blahnik, M. J., R. Ramanathan, C. R. Riley, and P. Minoo. 2001. Lipopolysaccharide-induced tumor necrosis factor-alpha and IL-10 production by lung macrophages from preterm and term neonates. *Pediatr Res* 50:726-731.
3. Shibata, Y., R. A. Henriksen, I. Honda, R. M. Nakamura, and Q. N. Myrvik. 2005. Splenic PGE2-releasing macrophages regulate Th1 and Th2 immune responses in mice treated with heat-killed BCG. *J Leukoc Biol* 78:1281-1290.
4. Shibata, Y., J. Gabbard, M. Yamashita, S. Tsuji, M. Smith, A. Nishiyama, R. A. Henriksen, and Q. N. Myrvik. 2006. Heat-killed BCG induces biphasic cyclooxygenase 2+ splenic macrophage formation--role of IL-10 and bone marrow precursors. *J Leukoc Biol* 80:590-598.
5. Nishiyama, A., S. Tsuji, M. Yamashita, R. A. Henriksen, Q. N. Myrvik, and Y. Shibata. 2006. Phagocytosis of N-acetyl-d-glucosamine particles, a Th1 adjuvant, by RAW 264.7 cells results in MAPK activation and TNF-alpha, but not IL-10, production. *Cell Immunol* 239:103-112.
6. Yamashita, M., T. Shinohara, S. Tsuji, Q. N. Myrvik, A. Nishiyama, R. A. Henriksen, and Y. Shibata. 2007. Catalytically Inactive Cyclooxygenase 2 and Absence of Prostaglandin E2 Biosynthesis in Murine Peritoneal Macrophages following In Vivo Phagocytosis of Heat-Killed Mycobacterium bovis Bacillus Calmette-Guerin. *J Immunol* 179:7072-7078.
7. Yamashita, M., S. Tsuji, A. Nishiyama, Q. N. Myrvik, R. A. Henriksen, and Y. Shibata. 2007. Differential subcellular localization of COX-2 in macrophages phagocytosing heat-killed Mycobacterium bovis BCG. *Am J Physiol Cell Physiol* 293:C184-190.

APPENDICES:

Appendix I:

Yamashita, M., T. Shinohara, S. Tsuji, Q. N. Myrvik, A. Nishiyama, R. A. Henriksen, and Y. Shibata. 2007. Catalytically Inactive Cyclooxygenase 2 and Absence of Prostaglandin E2 Biosynthesis in Murine Peritoneal Macrophages following In Vivo Phagocytosis of Heat-Killed Mycobacterium bovis Bacillus Calmette-Guerin. *J Immunol* 179:7072-7078, Task 2.

Appendix II:

Nishiyama A, T Shinohara, S Tsuji, M Yamashita,RA Henriksen, QN Myrvik, Y Shibata. Depletion of cellular cholesterol enhances macrophage MAPK activation by chitin microparticles but not by heat-killed *Mycobacterium bovis* BCG. *Am J Physiol Cell Physiol (in revision).* Task 3.

Catalytically Inactive Cyclooxygenase 2 and Absence of Prostaglandin E_2 Biosynthesis in Murine Peritoneal Macrophages following In Vivo Phagocytosis of Heat-Killed *Mycobacterium bovis* Bacillus Calmette-Guérin[1]

Makiko Yamashita,* Tsutomu Shinohara,* Shoutaro Tsuji,* Quentin N. Myrvik,† Akihito Nishiyama,* Ruth Ann Henriksen,‡ and Yoshimi Shibata[2]*

Over 25 years ago, it was observed that peritoneal macrophages (Mϕ) isolated from mice given heat-killed *Mycobacterium bovis* bacillus Calmette-Guérin (HK-BCG) i.p. did not release PGE_2. However, when peritoneal Mϕ from untreated mice are treated with HK-BCG in vitro, cyclooxygenase 2 (COX-2), a rate-limiting enzyme for PGE_2 biosynthesis, is expressed and the release of PGE_2 is increased. The present study of peritoneal Mϕ obtained from C57BL/6 mice and treated either in vitro or in vivo with HK-BCG was undertaken to further characterize the cellular responses that result in suppression of PGE_2 release. The results indicate that Mϕ treated with HK-BCG in vivo express constitutive COX-1 and inducible COX-2 that are catalytically inactive, are localized subcellularly in the cytoplasm, and are not associated with the nuclear envelope (NE). In contrast, Mϕ treated in vitro express catalytically active COX-1 and COX-2 that are localized in the NE and diffusely in the cytoplasm. Thus, for local Mϕ activated in vivo by HK-BCG, the results indicate that COX-1 and COX-2 dissociated from the NE are catalytically inactive, which accounts for the lack of PGE_2 production by local Mϕ activated in vivo with HK-BCG. Our studies further indicate that the formation of catalytically inactive COX-2 is associated with in vivo phagocytosis of HK-BCG, and is not dependent on extracellular mediators produced by in vivo HK-BCG treatment. This attenuation of PGE_2 production may enhance Mϕ-mediated innate and Th1-acquired immune responses against intracellular infections which are suppressed by PGE_2. *The Journal of Immunology,* 2007, 179: 7072–7078.

Phagocytosis of intracellular bacteria by macrophages (Mϕ)[3] results in cellular activation with expression of cyclooxygenase-2 (COX-2), a rate-limiting enzyme for PGE_2 biosynthesis. PGE_2 down-regulates innate and Th1-mediated immune responses induced by bacteria in autocrine and paracrine fashions. For example, PGE_2 inhibits inducible NO synthase/NO synthesis, NAPDH oxidase/superoxide anion release, and IL-12/IL-18/TNF-α synthesis (1–3). In contrast, PGE_2 promotes IL-10 production by Mϕ (4, 5), a Th1-to-Th2 shift of acquired immune responses (4, 5), dendritic cell Ag presentation (6), regulatory T cell differentiation and function (7), bone marrow progenitor cell migration via the CXCR4/stromal cell-derived factor-1 (CXCL12) system (8), IL-23 production (9), and Mϕ production of matrix metalloproteinase 9 (10). Regulation of these events, therefore, may depend on the regulation of PGE_2 release by COX-2^+ Mϕ (11). The formation of these PGE_2-releasing, activated Mϕ (PGE_2-Mϕ) appears to be regulated by multiple bacterial and host factors, including the tissue origin of the Mϕ (12–14).

Humes et al. (15) reported for the first time in 1980 that PGE_2 release by peritoneal Mϕ isolated from mice that are given heat-killed *Mycobacterium bovis* bacillus Calmette-Guérin (HK-BCG) or HK-*Corynebacterium parvum* (*Propionibacterium acnes*) i.p. is significantly reduced compared with that released by untreated peritoneal Mϕ. Studies by other groups including our own confirmed this phenomenon (13, 16, 17). Because peritoneal Mϕ elicited by i.p. HK-*C. parvum* in both monocytopenic and control mice show diminished PGE_2 biosynthesis, the phenomenon is not dependent on monocyte-derived Mϕ migration but rather is dependent on the direct interaction between local Mϕ and bacteria (13). A precise explanation for the suppression of PGE_2 release has not been established. In sharp contrast to long-held views, recent studies indicate that in vitro these bacteria induce COX-2 expression and PGE_2 biosynthesis by various Mϕ preparations including normal peritoneal Mϕ, blood monocytes, and Mϕ cell lines (18–26). Although the regulation of COX-1 and COX-2 expression has been extensively studied (27), exact mechanisms for regulation of PGE_2 biosynthesis by Mϕ activated with HK-BCG in vitro or in vivo are still unclear (12).

PGE_2 biosynthesis is initiated by activation of phospholipase A_2 (PLA_2) to release arachidonic acid (AA), which is metabolized by constitutive COX-1 and inducible COX-2 yielding PGH_2, which is converted to PGE_2 by cytosolic PGE synthase or microsomal

*College of Biomedical Sciences, Florida Atlantic University, Boca Raton, FL 33431; †Palmeto Dr, Caswell Beach, NC 28461; and ‡Department of Physiology, Brody School of Medicine, East Carolina University, Greenville, NC 27834

Received for publication April 30, 2007. Accepted for publication September 1, 2007.

The costs of publication of this article were defrayed in part by the payment of page charges. This article must therefore be hereby marked *advertisement* in accordance with 18 U.S.C. Section 1734 solely to indicate this fact.

[1] This work was supported by National Institutes of Health RO1 HL71711, Department of Defense DAMD 17-03-1-0004, the Charles E. Schmidt Biomedical Foundation (to Y.S.), and Florida Atlantic University.

[2] Address correspondence and reprint requests to Dr. Yoshimi Shibata, College of Biomedical Sciences, Florida Atlantic University, 777 Glades Road, P.O. Box 3091, Boca Raton, FL 33431-0991. E-mail address: yshibata@fau.edu

[3] Abbreviations used in this paper: Mϕ, macrophage; COX, cyclooxygenase; HK, heat killed; BCG, bacillus Calmette-Guérin; NE, nuclear envelope; ER, endoplasmic reticulum; PGES, PGE synthase; cPLA2, cytosolic phospholipase A2; PI, propidium iodide; AA, arachidonic acid; TMPD, *N,N,N′,N′*-tetramethyl-*p*-phenylenediamine; CFDA, carboxyfluorescein diacetate.

PGES (28, 29). Catalytically active COX-1 and COX-2 are localized in the nuclear envelop (NE) and endoplasmic reticulum (ER) of PGE_2-releasing cells (30–32). More recent studies have suggested that for functional coupling and PGE_2 biosynthesis, cytosolic PLA_2, COXs, and PGESs appear to be localized in the perinuclear region (28, 33).

Previously, we demonstrated that i.p. administration of HK-BCG results in at least two different forms of COX-2^+ splenic Mϕ: Mϕ obtained beginning at 1 day following HK-BCG treatment, which have catalytically inactive COX-2 dissociated from the NE and do not release PGE_2, and Mϕ obtained 7 days following treatment which have catalytically active COX-2 localized at the NE and release PGE_2. The dissociation of COX-2 from the NE is associated with in vivo phagocytosis of HK-BCG (34). Although capable of phagocytosis, the splenic Mϕ expressing catalytically active COX-2 do not contain intracellular HK-BCG (14, 34). Neither of these COX-2^+ Mϕ subsets can be induced in vitro, where only catalytically active COX-2^+ Mϕ are seen, and only in the presence of phagocytosed HK-BCG (34). Because formation of splenic and peritoneal PGE_2-Mϕ have distinct features (13), we sought to determine whether catalytically inactive COX-2 is induced in peritoneal Mϕ that phagocytose HK-BCG in vivo. We found that endogenous factors involved in phagocytosis of HK-BCG in vivo, but not extracellular signaling molecules produced locally by HK-BCG, are responsible for regulating the subcellular localization COX-2.

Materials and Methods

Animals

Nonpregnant female C57BL/6 mice, 8–14 wk old, were obtained from Harlan Breeders. Mice were maintained in barrier-filtered cages and fed Purina laboratory chow and tap water ad libitum. Experimental protocols used in this study were approved by the Institutional Animal Care and Use Committee at Florida Atlantic University.

*Intraperitoneal administration of HK-BCG, HK-*C. parvum*, or LPS*

As described previously (35), cultured *M. bovis* BCG Tokyo 172 strain were washed, autoclaved, and lyophilized. This HK-BCG powder was suspended in pyrogen-free saline and dispersed by brief (10 s) sonication immediately before use. These HK-BCG preparations contained undetectable levels of endotoxin (<0.03 endotoxin units/ml), as determined by the *Limulus* amebocyte lysate assay (Sigma-Aldrich) (35). Groups of mice (three per group) received 1, 0.1, or 0.01 mg of HK-BCG (5×10^8 bacilli/mg) i.p.. Controls received 0.1 ml of saline. Peritoneal lavage was performed at 6 or 24 h. As comparison controls, peritoneal Mϕ were also obtained from mice given 1 mg of HK-*C. parvum* (13) or 100 μg of LPS (*Escherichia coli*:0111:B4, phenol; Sigma-Aldrich) i.p. The schedules were identical with those used for HK-BCG.

*Peritoneal Mϕ preparation and treatment with HK-BCG, HK-*C. parvum*, or LPS in vitro*

Peritoneal lavage was performed as previously described (13). Nucleated peritoneal cells were counted in a Coulter counter (model Z1; Beckman Coulter). Differential cell counts were performed on cytospin preparations (Shandon Southern Instruments) stained with Diff-Quik. To enrich plastic-adherent Mϕ, peritoneal cells at 1×10^6 cells/ml suspended in RPMI 1640 plus 5% FBS were incubated in culture dishes (Falcon) for 2 h. Nonadherent cells (lymphocytes) were removed by washing with warmed medium. Adherent cells were cultured with 100 μg/ml HK-BCG, HK-*C. parvum*, or 1 μg/ml LPS for an additional 6 or 24 h. In some experiments, plasma and cell-free peritoneal lavage fluid isolated from the HK-BCG-treated mice were added to peritoneal Mϕ cultures with HK-BCG.

Cocultures of peritoneal Mϕ treated with HK-BCG in vitro and in vivo

Peritoneal Mϕ were labeled with 1 μM carboxyfluorescein diacetate (CFDA; Molecular Probes) at 37°C for 15 min and washed with RPMI 1640 plus 5% FBS. CFDA-labeled Mϕ (10^6 cells/ml) were cultured with 100 μg/ml HK-BCG for 6 h and mixed with peritoneal cells at 10^6 cells/ml isolated from mice in which 1 mg of HK-BCG was given i.p. 6 h before harvest. The mixed cells were cultured for an additional 18 h.

PGE_2 assay

For assay of PGE_2 release, plastic adherent peritoneal Mϕ (1×10^6 cells/ml) were cultured in serum-free RPMI 1640 with 1 μM calcium ionophore A23187 (Sigma-Aldrich) for 2 h. PGE_2 levels in the culture supernatants were measured by competitive ELISA (Cayman Chemical).

Subcellular localization of COX-1 and COX-2 by confocal microscopy

Peritoneal Mϕ prepared as described above were fixed with 4% paraformaldehyde in PBS for 30 min. The fixed cells were permeabilized with 0.1% Triton X-100 in PBS for 5 min and incubated in blocking buffer consisting of PBS with 10% FBS for 3 h at 22°C before incubation with anti-COX-1 or anti-COX-2 Ab (Cayman Chemical), 1:500 in blocking buffer, overnight at 4°C. Subsequently, cells were washed with PBS three times and incubated with FITC-conjugated donkey anti-rabbit IgG (1:500; Jackson ImmunoResearch Laboratories) for 1 h at 22°C. For detection of nuclei and HK-BCG, propidium iodine (PI) was mixed at 10 μg/ml with the secondary Ab solution. After washing three times, cells were examined with a laser scanning confocal microscope (Bio-Rad Radiance 2100). The images were processed with Adobe Photoshop software.

Subcellular fractionation

The method for subcellular fractionation was modified from that published previously (36). Peritoneal Mϕ prepared above were resuspended in 0.1 M Tris-HCl (pH 7.5), disrupted with a Dounce homogenizer, and forced through 26-gauge needles on ice. Disruption of cellular membranes was verified by microscopic examination. Cellular debris was removed by low-speed centrifugation ($700 \times g$ for 10 min), and the supernatants were further centrifuged at $10{,}000 \times g$ for 10 min to collect nuclei. The resulting supernatants were subjected to ultracentrifugation at $100{,}000 \times g$ for 90 min to isolate microsomal membrane and cytosolic fractions. Nuclear and membrane fractions were resuspended in 0.1 M Tris-HCl (pH 7.5). Protein concentrations were measured with a bicinchoninic acid assay (Pierce) and BSA as standard.

COX activity assay

The peroxidase component of COX in isolated cellular fractions was measured with a COX assay kit (Cayman Chemical) briefly as follows. The activity was determined with AA as a substrate and *N,N,N′,N′*-tetramethyl-*p*-phenylenediamine (TMPD) as cosubstrate. Equal amounts of protein (20 μg) were incubated at 25°C in a reaction mixture consisting of AA, TMPD, and heme in 0.1 M Tris-HCl (pH 7.5). The absorbance change, due to oxidation of TMPD during the initial 5 min, was measured at 590 nm. The specific enzyme activities were calculated and indicated as nanomoles per minute per milligram.

Western blot analysis

Peritoneal Mϕ, prepared as described above, were washed three times with cold saline. Washed cells were resuspended in lysis buffer (50 mM Tris-HCl (pH 7.5), 150 mM NaCl, 4 mM EDTA, 0.1% SDS, 1:500 protease inhibitor mixture (P8340; Sigma-Aldrich)), 1% Nonidet P-40, and 1% sodium deoxycholate). Debris was eliminated by centrifugation (10 min, $10{,}000 \times g$). Protein concentration in the lysate was measured with a bicinchoninic acid assay (Pierce) and BSA as standard. Equal amounts of protein from each sample were separated by SDS-PAGE. Proteins were then transferred to a polyvinylidene difluoride membrane (Millipore). The membrane was blocked with 10% nonfat dry milk and incubated with Abs (anti-COX-1, 1:2,000; anti-COX-2, 1:4,000 (Cayman Chemical); anti-GAPDH, 1:4,000 (Novus Biologicals) for the detection of GAPDH as constitutively expressed protein control) in 5% nonfat dry milk, overnight at 4°C. Following incubation with peroxidase-conjugated donkey anti-rabbit IgG (1:20,000; Jackson ImmunoResearch Laboratories), proteins were detected by chemiluminescence (ECL plus; Amersham) following the manufacturer's instructions.

Statistics

Data for PGE_2 release were analyzed by one-way ANOVA. For cell culture studies, tissues isolated from at least three mice were pooled unless indicated; these cells were cultured in at least triplicate in each group. Differences between mean values for the COX activity assays were analyzed by Student's *t* test with Statcel software. A value of $p < 0.05$ is considered statistically significant.

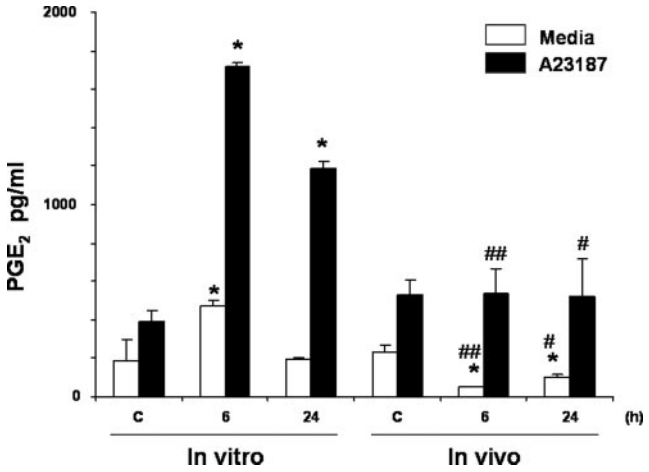

FIGURE 1. Differential PGE_2 biosynthesis by Mϕ treated in vitro or in vivo with HK-BCG. For in vivo HK-BCG treatment, groups of C57BL/6 mice received 1 mg of HK-BCG i.p. After 6 or 24 h, peritoneal lavage cells were harvested. For in vitro HK-BCG treatment, normal resident peritoneal Mϕ were incubated with 100 μg/ml HK-BCG for 6 or 24 h, and cells were harvested. C indicates cells exposed to saline for 24 h. To determine PGE_2 release, the Mϕ suspension (10^6/ml) was stimulated with 1 μM A23187 (■) or medium (□), for 2 h. PGE_2 was assayed by ELISA. Mean ± SD, $n = 3$. *, $p < 0.005$ compared with C (saline) in the same group. #, $p < 0.005$ and ##, $p < 0.0005$ compared with the corresponding in vitro group, respectively.

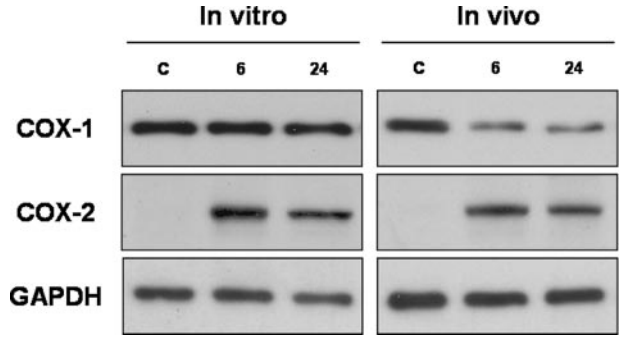

FIGURE 2. The detection of COX-1 and COX-2 in Mϕ treated in vitro or in vivo with HK-BCG. Peritoneal Mϕ treated in vivo or in vitro with HK-BCG were prepared as indicated in Fig. 1. COX-1, COX-2, and GAPDH were determined by Western blotting as indicated in *Materials and Methods*. GAPDH bands show equivalent loading of samples.

Results

Difference in PGE_2 release from peritoneal Mϕ treated in vivo or in vitro with HK-BCG

Intraperitoneal administration of 1 mg of HK-BCG was chosen to achieve an inflammatory response in mice like that associated with mycobacterial infection. This dose was also used previously to induce splenic PGE_2-Mϕ resulting in a Th1-to-Th2 shift of immune response (5). Previous in vitro studies showed that Mϕ phagocytose mycobacteria through TLR2 and that expression of COX-2 and PGE_2 biosynthesis are dependent on MAPK and NF-κB activation (19). Results shown in Fig. 1 indicate a difference in PGE_2 production by peritoneal Mϕ dependent on exposure to HK-BCG in vitro or in vivo. Calcium ionophore A23187-elicited production of PGE_2 by resident peritoneal Mϕ treated in vitro with HK-BCG is increased at 6 and 24 h, but is unchanged following in vivo treatment (Fig. 1, ■). At 6 h, the constitutive production of PGE_2 by peritoneal Mϕ treated in vitro with HK-BCG is also increased, but is suppressed for cells treated in vivo (Fig. 1, □).

Distinct subcellular localization of COX in Mϕ activated with HK-BCG in vivo and in vitro

We determined the COX levels in peritoneal Mϕ activated with HK-BCG in vivo and in vitro. As shown in Fig. 2, in vitro treatment of peritoneal Mϕ resulted in increased COX-2 levels, without a change in COX-1. In contrast, for Mϕ from mice treated with 1 mg of HK-BCG in vivo, an increase in COX-2 was accompanied by a decrease in COX-1 (Fig. 2). The results were similar at 6 and 24 h.

We further determined the subcellular localization of COX-2 by confocal microscopy. As shown in Fig. 3, Mϕ activated in vitro expressed COX-2 that was localized in the NE. In contrast, Mϕ activated in vivo had a dense form of COX-2 distributed in the cytoplasm, but not localized in the NE (Fig. 3). COX-1 in untreated Mϕ was consistently expressed in the NE and ER, which was not changed for Mϕ treated in vitro. However, when Mϕ were activated in vivo, COX-1 appeared as the dense form dissociated from the NE with a pattern similar to that seen for COX-2 (Fig. 4).

Differential COX distribution in Mϕ subcellular fractions

To further confirm that COX-2 dissociated from the NE is catalytically inactive, peritoneal Mϕ treated in vivo with 1 mg of HK-BCG were homogenized and subjected to differential centrifugation. For Mϕ activated in vitro, relatively more COX protein and activity were detected in the nuclear and membrane fractions than in the cytosolic fraction (Fig. 5). The profiles of COX-1 and COX-2 distribution are similar to previous reports using various PGE_2-releasing cells (36, 37). In contrast, COX protein isolated from Mϕ treated in vivo was predominantly detected in the membrane fraction (Fig. 5*A*), but the COX activity was not greater than the background level seen in the nuclear and cytosolic fractions (Fig. 5*B*).

Taken together, these results indicate that, following in vivo treatment with 1 mg of HK-BCG, COX-1 and COX-2 are dissociated from the NE and catalytically inactive. It appears that these

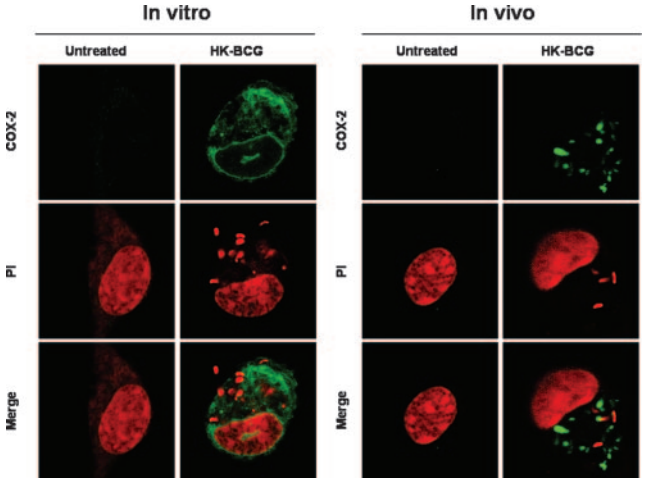

FIGURE 3. Subcellular localization of COX-2 in peritoneal Mϕ after HK-BCG treatment. Peritoneal Mϕ treated in vivo or in vitro with HK-BCG for 24 h were prepared as indicated in Fig. 1. Cells were examined by confocal microscopy following staining with anti-COX-2 (green) and PI (red) for the nucleus. HK-BCG is also stained by PI.

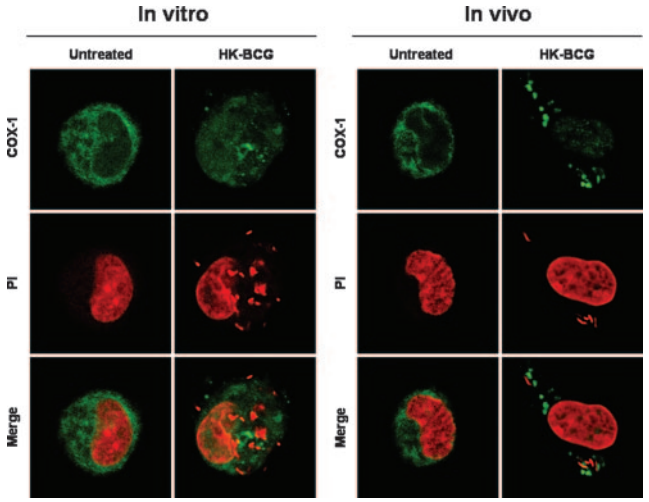

FIGURE 4. Subcellular localization of COX-1 in peritoneal Mϕ after HK-BCG treatment. Peritoneal Mϕ treated in vivo or in vitro with HK-BCG for 24 h were prepared as indicated in Fig. 1. Cells were examined by confocal microscopy following staining with anti-COX-1 (green) and PI (red) for the nucleus. HK-BCG is also stained by PI.

inactive forms may be associated with aggregation of COX protein. In contrast, peritoneal Mϕ exposed to HK-BCG in vitro expressed both COX protein and activity in the nuclear and membrane fractions.

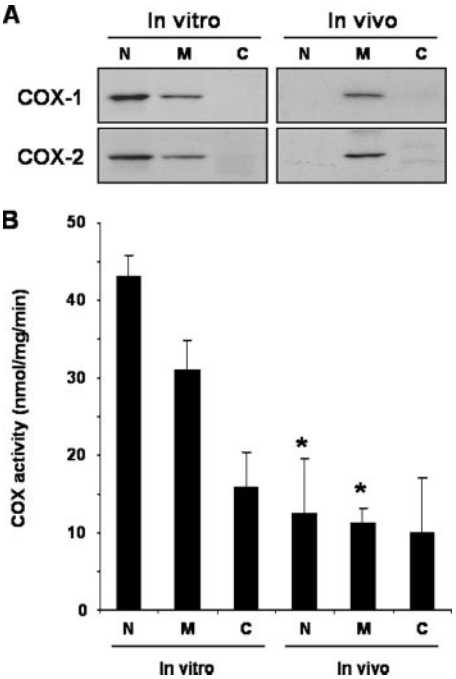

FIGURE 5. Distribution and activity of COX in subcellular fractions. Peritoneal Mϕ treated with HK-BCG in vitro or in vivo for 24 h as indicated in Fig. 1 were homogenized and separated into nuclear (N), membrane (M), and cytosolic (C) fractions by differential centrifugation as detailed in *Materials and Methods*. *A*, Protein (20 μg) in each fraction was used for COX-1 and COX-2 detection by Western blotting. *B*, The COX activity in each fraction was measured by using a COX assay kit (Cayman Chemical) following the manufacturer's instructions. The specific enzyme activities were calculated and indicated as nanomoles per minute per milligram. Mean ± SD, $n = 3$. *, $p < 0.001$ compared with the activity of the corresponding in vitro fraction.

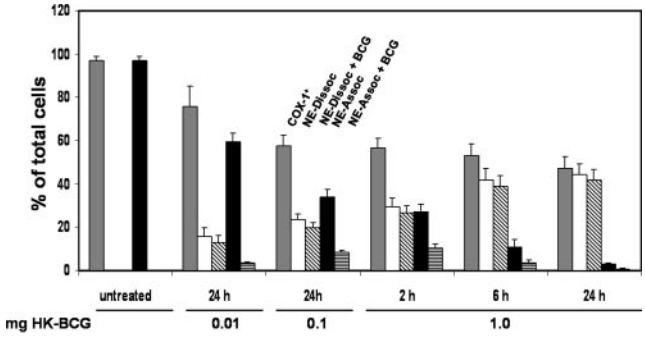

FIGURE 6. Time and HK-BCG dose dependence of COX-1 localization. Groups of C57BL/6 female mice (three per group) received 0.01, 0.1, or 1 mg of HK-BCG i.p. on day 0. Peritoneal lavage cells were harvested at times indicated. Subcellular localization of COX-1 as well as identification of intracellular HK-BCG were performed by confocal microscopy as described under *Materials and Methods*. Mean ± SE, $n = 3$. Percentage of COX-1$^+$ Mϕ (▨), percentage of Mϕ with NE-dissociated COX-1 (□), percentage of Mϕ with NE-dissociated COX-1 and PI-stained BCG (▧), percentage of Mϕ with NE-associated COX-1 (■), and percentage of Mϕ with NE-associated COX-1 and PI-stained BCG (▤).

Kinetics of COX localization and phagocytosis of HK-BCG

To determine the kinetics of the subcellular translocation of COX-1 and expression of COX-2, peritoneal Mϕ were harvested at 2, 6, and 24 h after i.p. administration of 1 mg of HK-BCG. The localization of COX-1 and COX-2 in each sample was analyzed by confocal microscopy. Fig. 6 shows that 97% of untreated peritoneal Mϕ expressed COX-1, whereas COX-1$^+$ Mϕ were reduced to 56, 53, and 47% at 2, 6, and 24 h after treatment with 1 mg of HK-BCG. This reduction corresponds to the reduced COX-1 protein levels determined by Western blot (Fig. 2). The percentage of COX-1 present in the NE-dissociated dense form increased from 52% (30% of total cells) at 2 h until at 24 h nearly all COX-1 (44% of total cells) was in this form. Interestingly, ≥90% of the NE-dissociated (dense form) COX-1$^+$ Mϕ had phagocytosed HK-BCG that was stained by PI (Fig. 6). We previously demonstrated that HK-BCG stained with PI are almost totally costained with anti-BCG Abs (34).

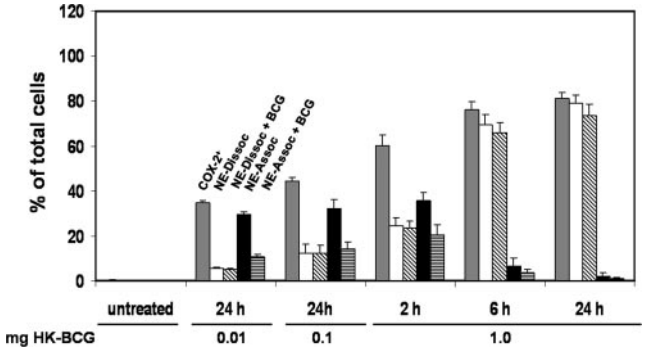

FIGURE 7. Time and HK-BCG dose dependence of COX-2 localization. Groups of C57BL/6 female mice (three per group) received 0.01, 0.1, or 1 mg of HK-BCG i.p. on day 0. Peritoneal lavage cells were harvested at times indicated. Subcellular localization of COX-2 as well as identification of intracellular HK-BCG were performed by confocal microscopy as described under *Materials and Methods*. Mean ± SE, $n = 3$. Percentage of COX-2$^+$ Mϕ (▨), percentage of Mϕ with NE-dissociated COX-2 (□), percentage of Mϕ with NE-dissociated COX-2$^+$ and PI-stained BCG (▧), percentage of Mϕ with NE-associated COX-2 (■), and percentage of Mϕ with NE-associated COX-2 and PI-stained BCG (▤).

Table I. *The effects of peritoneal fluid isolated from HK-BCG-treated mice on the localization of COX-2 in vitro*

Cocultures		COX-2 Localization[a]	
Responders with HK-BCG in vitro[b]	Additive from HK-BCG-treated mice[c]	CFDA-Mϕ	Unlabeled Mϕ
Unlabeled Mϕ	RPMI 1640	N/A	100% NE associated
Unlabeled Mϕ	Peritoneal fluid	N/A	100% NE associated
Unlabeled Mϕ	Sera	N/A	100% NE associated
CFDA Mϕ	Peritoneal cells	100% NE associated	100% NE dissociated

[a] Cells were stained with Ab to COX-2 and examined by confocal microscopy. Percentage of COX-2$^+$ Mϕ with NE-associated COX-2 or with NE-dissociated COX-2 is indicated.

[b] Peritoneal Mϕ at 10^6 cells/ml were labeled in vitro with CFDA or media (unlabeled), and stimulated with 100 μg/ml HK-BCG for 6 h before transferring additive.

[c] Mice received 1 mg of HK-BCG i.p. After 6 h, peritoneal lavage was performed with 1 ml of cold serum-free RPMI 1640 and the lavage fluid was centrifuged to isolate cells from the peritoneal fluid. Sera were also harvested. As stimulators, 10^6 peritoneal cells/ml, 20% peritoneal fluid or 20% sera were added to the in vitro responder cells. These mixtures were cultured for an additional 18 h.

COX-2, which was present in <1% of untreated cells, was seen in 60% of Mϕ at 2 h with the NE-dissociated dense form present in 41% of these cells (25% of total cells) (Fig. 7). These NE-dissociated (dense form) COX-2$^+$ cells increased to >90% of COX-2$^+$ cells (70% of total cells) at 6 h. As for COX-1, most (95, 95, and 93% at 2, 6, and 24 h, respectively) of Mϕ expressing NE-dissociated COX-2 contained intracellular PI-stained HK-BCG. Figs. 6 and 7 also show that, at 24 h, COX-1 was lost from half of the cells originally containing COX-1, and at the same time 81% of cells now express COX-2. The results further suggest that some cells contain both isoforms of COX.

Dose dependence of COX localization

The subcellular translocation of COX-1 and localization of COX-2 were also investigated at lower doses of HK-BCG (0.1 or 0.01 mg). The results shown in Fig. 6 indicate that the fractions of Mϕ-expressing COX-1 and NE-associated COX-1 are both reduced dose dependently at 24 h. Intracellular HK-BCG was detected in over 80% of NE-dissociated (dense form) COX-1$^+$ Mϕ (Fig. 6). Our results clearly indicate that the NE-dissociated (dense form) COX-1 pattern is associated with phagocytosis of HK-BCG.

At 24 h, there were 44 or 35% COX-2$^+$ Mϕ in response to 0.1 or 0.01 mg of HK-BCG, respectively, compared with 81% at 1 mg of HK-BCG (Fig. 7). Mϕ with NE-dissociated (dense form) COX-2 increased dose-dependently to 98% of total COX-2$^+$ Mϕ at 1 mg of HK-BCG. At all doses, nearly all of these NE-dissociated COX-2$^+$ cells contained PI-stained intracellular HK-BCG. Although this was the predominant COX-2$^+$ phenotype in response to 1 mg of HK-BCG at 24 h, there were a few cells observed with NE-associated COX-2 containing HK-BCG (Fig. 7). Thus, in vivo treatment with 1 mg of HK-BCG resulted in a dramatic shift from NE-associated COX-1 to NE-dissociated and catalytically inactive COX-2 at 24 h.

*Intraperitoneal administration of HK-*C. parvum *and LPS induces NE-dissociated and -associated COX-2, respectively, in peritoneal Mϕ*

Additional studies following intraperitoneal administration of bacterial endotoxin (LPS) or HK-*C. parvum* showed that soluble LPS induced catalytically active NE-associated COX-2, and HK-*C. parvum* induced catalytically inactive, NE-dissociated COX-2 at 24 h (data not shown). These results further support the conclusion that NE-dissociated (dense form) COX-2 expression depends on phagocytosis.

The effects of peritoneal fluid isolated from HK-BCG-treated mice on localization of COX-2 in vitro

Our results suggest that extracellular factors produced by in vivo HK-BCG treatment regulates the localization of COX-2 in peritoneal Mϕ. To test this hypothesis, CFDA-labeled or unlabeled normal peritoneal Mϕ were challenged with HK-BCG and cocultured with peritoneal cells, cell-free peritoneal fluid, or sera isolated from HK-BCG-treated mice. All CFDA-labeled Mϕ expressed NE-associated COX-2 in response to HK-BCG in vitro and the localization was unchanged by coculture with peritoneal cells, peritoneal fluid, or sera from HK-BCG-treated mice (Table I) or from normal mice (data not shown). Thus, it appears that extracellular mediators produced by HK-BCG treatment in vivo do not induce the NE-dissociated form of COX-2 in Mϕ treated in vitro with HK-BCG.

Discussion

NE-dissociated COX

It is well-established that catalytically active COX-2 is localized in the NE/ER of activated human monocytes and umbilical vein endothelial cells, as well as murine NIH 3T3 cells, and splenic Mϕ, where it mediates PGE_2 biosynthesis (30–32, 34). However, our present and previous studies (34) demonstrate that most splenic and peritoneal Mϕ isolated from mice 24 h after receiving 1 mg of HK-BCG i.p. express catalytically inactive COX-2. This inactive COX-2 appears as a densely stained structure and is completely dissociated from the NE. Constitutively expressed COX-1 is also detected in a dense form dissociated from the NE in these Mϕ. Thus, catalytically inactive forms of COX-1 and COX-2 are present, without PGE_2 biosynthesis, in activated splenic (34) and peritoneal Mϕ. However, it is of particular note that the stimulation of normal Mϕ with HK-BCG in vitro results in expression of catalytically active COX-2, which is localized in the NE/ER. Therefore, factors induced in vivo by HK-BCG administration are obligatory for establishing the catalytically inactive form of COX and consequently the regulation of PG production.

Role of phagocytosis

Another provocative finding is that intracellular HK-BCG is observed in nearly all NE-dissociated COX-2$^+$ peritoneal Mϕ isolated from mice 24 h after i.p. administration of HK-BCG (Fig. 7). Thus, phagocytosis of HK-BCG in the local tissues is significantly associated with expression of the NE-dissociated COX-2, although there are a few COX-2$^+$ Mϕ without intracellular HK-BCG and a

few COX-2$^-$ Mϕ with intracellular HK-BCG in the same samples. These and our earlier studies indicate that the in vivo phagocytosis of HK-BCG by Mϕ in various tissues results in the formation of catalytically inactive COX-2. In preliminary studies in which HK-BCG was administered intranasally, this phenomenon was also demonstrated in alveolar Mϕ (data not shown). However, for mice receiving lower doses of HK-BCG, Mϕ subsets with NE-associated (active) COX-2 and intracellular HK-BCG are present in relatively greater numbers in peritoneal Mϕ (Fig. 7). In contrast, peritoneal Mϕ activated in vitro with HK-BCG show only NE/ER-associated, catalytically active COX-2 with intracellular HK-BCG.

Furthermore, our studies with peritoneal Mϕ in culture (Table I) do not support the hypothesis that extracellular factors produced in response to HK-BCG in the peritoneal cavity or present in sera regulate the subcellular localization of COX isozymes. Thus, it appears that other endogenous factors associated with phagocytosis in vivo but not in vitro are important for the formation of catalytically inactive COX-2. Because the coculture studies presented in Table I were performed for only one set of time intervals, it is possible that, for instance, the early transient expression of a particular cellular mediator is critical for regulating the subcellular location of COX and its activity.

As presented in Fig. 5, the membrane (M) fraction from the Mϕ treated in vivo has less COX activity than the same fraction taken from cells treated in vitro, despite almost equivalent COX protein levels. This suggests that either 1) the COX isozymes in the membrane fractions of the cells treated in vivo have been structurally modified, rendering them less active, or 2) there is a nonstructural (biochemical) basis for this difference. One possibility is that the reduction/oxidation (redox) states of the membrane fractions differ between Mϕ exposed to HK-BCG in vivo and those exposed in vitro. The activities of both COX-1 and COX-2 are modulated by ambient hydroperoxide availability (38). It may be speculated that the sequestered NE-dissociated COX found in peritoneal Mϕ from HK-BCG-treated mice is, at least in part, a consequence of a low "peroxide tone" which limits COX activity.

COX localization in other studies

Other recent studies indicate that COX-2 localizes not only to the NE but also other subcellular sites. D'Avila et al. (39) have reported that intrapleural administration of live BCG induces lipid-laden pleural Mϕ in a TLR2-dependent but phagocytosis-independent manner. In these Mϕ, COX-2 is expressed and localized at lipid bodies within 24 h, and mediates a large amount of PGE_2 synthesis. For phorbol ester (PMA)-stimulated bovine aortic endothelial cells, Liou et al. (40) found that COX-2 is present in cytosolic vesicle-like structures, and that PGI_2 synthesis by these cells is not enhanced. In PMA- and IL-1β-treated fibroblasts, catalytically active COX-2 is found in the plasma membrane colocalized with caveolin (41). Girotti et al. (42) indicated that catalytically active COX-2 is localized in the phagosomes of peritoneal Mϕ after in vitro phagocytosis of zymosan particles. The localization of $cPLA_{2\alpha}$ followed by COX-2 to the phagosome correlated with the time course of PGE_2 production, suggesting that the phagosome membrane may serve as a site for release of AA and prostanoid production. However, the magnitudes of PGE_2 biosynthesis at the phagosome and NE were not reported (42). It is predicted that without colocalization of COX-2, $cPLA_{2\alpha}$, and PGES, PGE_2 synthesis does not occur and COX-2 is apparently inactive. Thus, regulation of COX-2 activity associated with its subcellular localization appears to be complex, dependent on cell types and specific activating agents.

COX-2 is not associated with phagosome

In our study using Mϕ activated in vivo, the dense form of COX-2 does not appear to be directly associated with intracellular HK-BCG (Fig. 3) or lysosome-associated membrane protein 1-positive late phagosomes (data not shown). Furthermore, activation of Mϕ in vitro also indicated that there is no direct association of COX-2 with intracellular HK-BCG (Fig. 3). Spencer et al. (36) demonstrated in their mutation analysis of COXs that the mutant proteins, which lack membrane binding domains and enzyme activity, are distributed in the microsomal fraction. They suggested that these mutant proteins are mostly present as unfolded aggregates. Although the membrane-binding domains of COX-1 and COX-2 appear to be important for maintaining their catalytic activity, the mechanisms underlying NE dissociation and enzyme inactivation are still unknown.

Role of COX-2 localization

In response to bacterial components, Mϕ become bactericidal with increases in NADPH oxidase/superoxide anion release, inducible NO synthase/NO production, and IL-12/TNF-α synthesis. PGE_2 down-regulates Th1 responses and bactericidal activity toward intracellular organisms. It is therefore reasonable to speculate that catalytically inactive COX-2$^+$ Mϕ enhance the development of bactericidal activities more effectively than Mϕ with catalytically active COX-2. In our studies, at 24 h following treatment with 1 mg of HK-BCG, both COX-1 and COX-2 are NE dissociated and inactive. Compartmentalization of COX might aid the development of bactericidal activity by placing this enzyme in a location where catalysis cannot occur. Whether additional posttranslational modification is involved in this regulation of COX activity is not known.

Conclusion

Our present and previous findings (12, 34) indicate that normal peritoneal and splenic Mϕ treated with HK-BCG in vitro express catalytically active COX-2 and release increased amounts of PGE_2 within 24 h. However, administration of HK-BCG activates various tissue Mϕ locally and systemically to express either catalytically active or inactive COX-2, dependent on route of administration, dose, timing, in vivo phagocytosis and the presence of bone marrow-derived PGE_2-Mϕ progenitors, which localize and mature at inflammatory sites. Although more studies are needed to elucidate regulatory mechanisms for the diversity of COX-2$^+$ Mϕ formation in vivo, it appears that the distinct COX-2$^+$ Mϕ subsets may play pro- and anti- inflammatory roles.

Disclosures

The authors have no financial conflict of interest.

References

1. van der Pouw Kraan, T. C., L. C. Boeije, R. J. Smeenk, J. Wijdenes, and L. A. Aarden. 1995. Prostaglandin-E_2 is a potent inhibitor of human interleukin 12 production. *J. Exp. Med.* 181: 775–779.
2. Harbrecht, B. G., Y. M. Kim, E. A. Wirant, R. L. Simmons, and T. R. Billiar. 1997. Timing of prostaglandin exposure is critical for the inhibition of LPS- or IFN-γ-induced macrophage NO synthesis by PGE2. *J. Leukocyte Biol.* 61: 712–720.
3. Pillinger, M. H., M. R. Philips, A. Feoktistov, and G. Weissmann. 1995. cross-talk in signal transduction via EP receptors: prostaglandin E_1 inhibits chemoattractant-induced mitogen-activated protein kinase activity in human neutrophils. *Adv. Prostaglandin Thromboxane Leukot. Res.* 23: 311–316.
4. Shinomiya, S., H. Naraba, A. Ueno, I. Utsunomiya, T. Maruyama, S. Ohuchida, F. Ushikubi, K. Yuki, S. Narumiya, Y. Sugimoto, et al. 2001. Regulation of TNFα and interleukin-10 production by prostaglandins I_2 and E_2: studies with prostaglandin receptor-deficient mice and prostaglandin E-receptor subtype-selective synthetic agonists. *Biochem. Pharmacol.* 61: 1153–1160.
5. Shibata, Y., R. A. Henriksen, I. Honda, R. M. Nakamura, and Q. N. Myrvik. 2005. Splenic PGE_2-releasing macrophages regulate Th1 and Th2 immune responses in mice treated with heat-killed BCG. *J. Leukocyte Biol.* 78: 1281–1290.

6. Vassiliou, E., V. Sharma, H. Jing, F. Sheibanie, and D. Ganea. 2004. Prostaglandin E_2 promotes the survival of bone marrow-derived dendritic cells. *J. Immunol.* 173: 6955–6964.
7. Baratelli, F., Y. Lin, L. Zhu, S. C. Yang, N. Heuze-Vourc'h, G. Zeng, K. Reckamp, M. Dohadwala, S. Sharma, and S. M. Dubinett. 2005. Prostaglandin E_2 induces FOXP3 gene expression and T regulatory cell function in human $CD4^+$ T cells. *J. Immunol.* 175: 1483–1490.
8. Salcedo, R., X. Zhang, H. A. Young, N. Michael, K. Wasserman, W. H. Ma, M. Martins-Green, W. J. Murphy, and J. J. Oppenheim. 2003. Angiogenic effects of prostaglandin E_2 are mediated by up-regulation of CXCR4 on human microvascular endothelial cells. *Blood* 102: 1966–1977.
9. Sheibanie, A. F., I. Tadmori, H. Jing, E. Vassiliou, and D. Ganea. 2004. Prostaglandin E_2 induces IL-23 production in bone marrow-derived dendritic cells. *FASEB J.* 18: 1318–1320.
10. Pavlovic, S., B. Du, K. Sakamoto, K. M. Khan, C. Natarajan, R. M. Breyer, A. J. Dannenberg, and D. J. Falcone. 2006. Targeting prostaglandin E_2 receptors as an alternative strategy to block cyclooxygenase-2-dependent extracellular matrix-induced matrix metalloproteinase-9 expression by macrophages. *J. Biol. Chem.* 281: 3321–3328.
11. Dubois, R. N., S. B. Abramson, L. Crofford, R. A. Gupta, L. S. Simon, L. B. Van De Putte, and P. E. Lipsky. 1998. Cyclooxygenase in biology and disease. *FASEB J.* 12: 1063–1073.
12. Shibata, Y., J. Gabbard, M. Yamashita, S. Tsuji, M. Smith, A. Nishiyama, R. A. Henriksen, and Q. N. Myrvik. 2006. Heat-killed BCG induces biphasic cyclooxygenase 2^+ splenic macrophage formation–role of IL-10 and bone marrow precursors. *J. Leukocyte Biol.* 80: 590–598.
13. Shibata, Y., A. P. Bautista, S. N. Pennington, J. L. Humes, and A. Volkman. 1987. Eicosanoid production by peritoneal and splenic macrophages in mice depleted of bone marrow by 89Sr. *Am. J. Pathol.* 127: 75–82.
14. Shibata, Y., and A. Volkman. 1985. The effect of bone marrow depletion on prostaglandin E-producing suppressor macrophages in mouse spleen. *J. Immunol.* 135: 3897–3904.
15. Humes, J. L., S. Burger, M. Galavage, F. A. Kuehl, Jr., P. D. Wightman, M. E. Dahlgren, P. Davies, and R. J. Bonney. 1980. The diminished production of arachidonic acid oxygenation products by elicited mouse peritoneal macrophages: possible mechanisms. *J. Immunol.* 124: 2110–2116.
16. Tripp, C. S., E. R. Unanue, and P. Needleman. 1986. Monocyte migration explains the changes in macrophage arachidonate metabolism during the immune response. *Proc. Natl. Acad. Sci. USA* 83: 9655–9659.
17. Fels, A. O., N. A. Pawlowski, E. L. Abraham, and Z. A. Cohn. 1986. Compartmentalized regulation of macrophage arachidonic acid metabolism. *J. Exp. Med.* 163: 752–757.
18. Tse, H. M., S. I. Josephy, E. D. Chan, D. Fouts, and A. M. Cooper. 2002. Activation of the mitogen-activated protein kinase signaling pathway is instrumental in determining the ability of *Mycobacterium avium* to grow in murine macrophages. *J. Immunol.* 168: 825–833.
19. Pathak, S. K., A. Bhattacharyya, S. Pathak, C. Basak, D. Mandal, M. Kundu, and J. Basu. 2004. Toll-like receptor 2 and mitogen- and stress-activated kinase 1 are effectors of *Mycobacterium avium*-induced cyclooxygenase-2 expression in macrophages. *J. Biol. Chem.* 279: 55127–55136.
20. Eriks, I. S., and C. L. Emerson. 1997. Temporal effect of tumor necrosis factor α on murine macrophages infected with *Mycobacterium avium. Infect. Immun.* 65: 2100–2106.
21. Maw, W. W., T. Shimizu, K. Sato, and H. Tomioka. 1997. Further study on the roles of the effector molecules of immunosuppressive macrophages induced by mycobacterial infection in expression of their suppressor function against mitogen-stimulated T cell proliferation. *Clin. Exp. Immunol.* 108: 26–33.
22. Cross, M. L., L. J. Slobbe, G. S. Buchan, and J. F. Griffin. 1996. In vitro responses of cervine macrophages to bacterial stimulants. *Vet. Immunol. Immunopathol.* 53: 249–256.
23. Venkataprasad, N., H. Shiratsuchi, J. L. Johnson, and J. J. Ellner. 1996. Induction of prostaglandin E_2 by human monocytes infected with *Mycobacterium avium* complex–modulation of cytokine expression. *J. Infect. Dis.* 174: 806–811.
24. Rastogi, N., M. Bachelet, and J. P. Carvalho de Sousa. 1992. Intracellular growth of *Mycobacterium avium* in human macrophages is linked to the increased synthesis of prostaglandin E_2 and inhibition of the phagosome-lysosome fusions. *FEMS Microbiol. Immunol.* 4: 273–279.
25. Keller, R., R. Keist, and P. H. van der Meide. 1991. Modulation of tumoricidal activity, induced in bone-marrow-derived mononuclear phagocytes by interferon γ or *Corynebacterium parvum*, by interferon β, tumor necrosis factor, prostaglandin E_2, and transforming growth factor β. *Int. J. Cancer* 49: 796–800.
26. Uchiya, K., and T. Nikai. 2004. *Salmonella enterica* serovar *typhimurium* infection induces cyclooxygenase 2 expression in macrophages: involvement of *Salmonella* pathogenicity island 2. *Infect. Immun.* 72: 6860–6869.
27. Smith, W. L., D. L. DeWitt, and R. M. Garavito. 2000. Cyclooxygenases: structural, cellular, and molecular biology. *Annu. Rev. Biochem.* 69: 145–182.
28. Murakami, M., H. Naraba, T. Tanioka, N. Semmyo, Y. Nakatani, F. Kojima, T. Ikeda, M. Fueki, A. Ueno, S. Oh, and I. Kudo. 2000. Regulation of prostaglandin E_2 biosynthesis by inducible membrane-associated prostaglandin E_2 synthase that acts in concert with cyclooxygenase-2. *J. Biol. Chem.* 275: 32783–32792.
29. Uematsu, S., M. Matsumoto, K. Takeda, and S. Akira. 2002. Lipopolysaccharide-dependent prostaglandin E_2 production is regulated by the glutathione-dependent prostaglandin E_2 synthase gene induced by the Toll-like receptor 4/MyD88/NF-IL6 pathway. *J. Immunol.* 168: 5811–5816.
30. Otto, J. C., and W. L. Smith. 1994. The orientation of prostaglandin endoperoxide synthases-1 and -2 in the endoplasmic reticulum. *J. Biol. Chem.* 269: 19868–19875.
31. Morita, I., M. Schindler, M. K. Regier, J. C. Otto, T. Hori, D. L. DeWitt, and W. L. Smith. 1995. Different intracellular locations for prostaglandin endoperoxide H synthase-1 and -2. *J. Biol. Chem.* 270: 10902–10908.
32. Spencer, A. G., J. W. Woods, T. Arakawa, I. I. Singer, and W. L. Smith. 1998. Subcellular localization of prostaglandin endoperoxide H synthases-1 and -2 by immunoelectron microscopy. *J. Biol. Chem.* 273: 9886–9893.
33. Murakami, M., K. Nakashima, D. Kamei, S. Masuda, Y. Ishikawa, T. Ishii, Y. Ohmiya, K. Watanabe, and I. Kudo. 2003. Cellular prostaglandin E_2 production by membrane-bound prostaglandin E synthase-2 via both cyclooxygenases-1 and -2. *J. Biol. Chem.* 278: 37937–37947.
34. Yamashita, M., S. Tsuji, A. Nishiyama, Q. N. Myrvik, R. A. Henriksen, and Y. Shibata. 2007. Differential subcellular localizations of COX-2 by macrophages phagocytosing heat-killed *Mycobacterium bovis* BCG in vivo. *Am. J. Physiol.* 293: C184–C190.
35. Shibata, Y., I. Honda, J. P. Justice, M. R. Van Scott, R. M. Nakamura, and Q. N. Myrvik. 2001. Th1 adjuvant *N*-acetyl-D-glucosamine polymer up-regulates Th1 immunity but down-regulates Th2 immunity against a mycobacterial protein (MPB-59) in interleukin-10-knockout and wild-type mice. *Infect. Immun.* 69: 6123–6130.
36. Spencer, A. G., E. Thuresson, J. C. Otto, I. Song, T. Smith, D. L. DeWitt, R. M. Garavito, and W. L. Smith. 1999. The membrane binding domains of prostaglandin endoperoxide H synthases 1 and 2: peptide mapping and mutational analysis. *J. Biol. Chem.* 274: 32936–32942.
37. Patel, R., M. G. Attur, M. Dave, S. B. Abramson, and A. R. Amin. 1999. Regulation of cytosolic COX-2 and prostaglandin E_2 production by nitric oxide in activated murine macrophages. *J. Immunol.* 162: 4191–4197.
38. Kulmacz, R. J. 2005. Regulation of cyclooxygenase catalysis by hydroperoxides. *Biochem. Biophys. Res. Commun.* 338: 25–33.
39. D'Avila, H., R. C. Melo, G. G. Parreira, E. Werneck-Barroso, H. C. Castro-Faria-Neto, and P. T. Bozza. 2006. *Mycobacterium bovis* bacillus Calmette-Guérin induces TLR2-mediated formation of lipid bodies: intracellular domains for eicosanoid synthesis in vivo. *J. Immunol.* 176: 3087–3097.
40. Liou, J. Y., S. K. Shyue, M. J. Tsai, C. L. Chung, K. Y. Chu, and K. K. Wu. 2000. Colocalization of prostacyclin synthase with prostaglandin H synthase-1 (PGHS-1) but not phorbol ester-induced PGHS-2 in cultured endothelial cells. *J. Biol. Chem.* 275: 15314–15320.
41. Liou, J. Y., W. G. Deng, D. W. Gilroy, S. K. Shyue, and K. K. Wu. 2001. Colocalization and interaction of cyclooxygenase-2 with caveolin-1 in human fibroblasts. *J. Biol. Chem.* 276: 34975–34982.
42. Girotti, M., J. H. Evans, D. Burke, and C. C. Leslie. 2004. Cytosolic phospholipase A2 translocates to forming phagosomes during phagocytosis of zymosan in macrophages. *J. Biol. Chem.* 279: 19113–19121.

Depletion of cellular cholesterol enhances macrophage MAPK activation by chitin microparticles but not by heat-killed *Mycobacterium bovis* BCG

Akihito Nishiyama, * Tsutomu Shinohara,* Traci Pantuso, * Shoutaro Tsuji,* Makiko Yamashita,* Shizuka Shinohara,* Quentin N. Myrvik, † Ruth Ann Henriksen, ‡ and Yoshimi Shibata[1]*

* Department of Biomedical Sciences, Florida Atlantic University, Boca Raton, FL 33431-0991; ‡ Department of Physiology, Brody School of Medicine at East Carolina University, Greenville, NC 27834; † Caswell Beach, NC 28465

[1] Address correspondence and reprint requests to Yoshimi Shibata, Ph.D., College of Biomedical Sciences, Florida Atlantic University, 777 Glades Rd., Boca Raton, FL 33431-0991. Phone: (561) 297-0606. Fax: (561) 297-2221. E-mail: yshibata@fau.edu.

Running Title: Cholesterol-dependent MØ activation

Key words: *N*-acetyl-D-glucosamine polymer particles, cholesterol, phagosome formation, MAPK activation, Th1 cytokines, IL-10, COX-2

ABSTRACT

When macrophages phagocytose chitin (*N*-acetyl-D-glucosamine polymer) microparticles, MAPK are immediately activated in a manner dependent on phagosome formation, followed by the release of Th1 cytokines, but not IL-10. To determine whether phagocytosis and macrophage activation in response to chitin microparticles are dependent on membrane cholesterol, RAW264.7 macrophages were treated with methyl-β-cytodextrin (MBCD) to remove membrane cholesterol and stimulated with chitin and bacterial components including two heat-killed (HK) microorganisms and an oligodeoxynucleotide of bacterial DNA (CpG-ODN) as comparison controls. The treatment did not alter chitin binding or the phagocytosis of chitin particles 20 min after stimulation. At the same time, however, chitin-induced phosphorylation of cellular MAPK was accelerated and enhanced in an MBCD dose dependent manner. The increased phosphorylation was also observed for chitin phagosome-associated p38 and ERK1/2. In contrast, CpG-ODN, HK-*Mycobacterium bovis* BCG or HK-*Listeria monocytogenes* induced activation of MAPK in MBCD-treated cells at levels comparable to, or only slightly more than, those of control cells. We also found that MBCD treatment enhanced the production of TNF-α and the expression of cyclooxygenase 2 (COX-2) in response to chitin microparticles. In neither MBCD- nor saline- treated macrophages, did chitin particles induce detectable IL-10 mRNA synthesis. CpG-ODN-induced MAPK phosphorylation, TNF-α production, and COX-2 expression were less sensitive to MBCD treatment. Among the inanimate particles studied, our results indicate that macrophage activation by chitin microparticles was most sensitive to cholesterol depletion, suggesting that membrane structures integrated by cholesterol are important for physiologic regulation of chitin microparticle-induced cellular activation.

INTRODUCTION

Mononuclear phagocytes (M∅) provide the first immunologic line of defense through phagocytosis of microorganisms, apoptotic cells and inanimate particles, but responses differ among these agonists dependent primarily on engagement of different plasma membrane receptors (6, 14, 35). Our previous studies (18, 29) indicate that phagocytosis of chitin microparticles (1 – 10 μm *N*-acetyl-D-glucosamine [GlcNAc] polymer particles), a seemingly inert molecule, by murine MØ results in the activation of MAPK (p38, ERK1/2, JNK) followed by the development of innate immunity and promotion of acquired immune responses that mediate cellular activation of Type 1 helper lymphocytes (Th1) and M∅. Unlike bacterial Th1 adjuvants including heat-killed *Mycobacterium bovis* BCG (HK-BCG), bacterial endotoxin and CpG oligonucleotides (CpG-ODN), chitin microparticles do not induce IL-10, a Th2 cytokine that down-regulates Th1 adjuvant activity (18, 28, 29). Therefore, chitin microparticles may be considered a unique and clinically useful Th1 adjuvant (25, 28).

However, M∅ activation does not occur when chitin phagocytosis is inhibited by cytochalasin D (actin polymerization inhibitor), or in response to soluble chitin or non-phagocytosable (>50 μm) chitin (18, 29). Thus, although GlcNAc recognition is required, internalization/phagosome formation during the phagocytosis of chitin microparticles are also necessary for the observed MAPK activation and development of a Th1 response (18, 29). Literature indicates that membrane lipids including cholesterol are likely instrumental in the remodeling of the actin cytoskeleton and in directing membrane traffic during the formation and maturation of

phagosomes (39). We have further determined whether phagocytosis of chitin microparticles resulting in early MAPK activation is dependent on membrane cholesterol.

Methyl-β-cyclodextrin (MBCD) removes plasma membrane cholesterol through formation of a soluble complex with cholesterol that results in disruption of plasma membrane detergent-resistant cholesterol-rich microdomains (DRM) including caveolae and lipid rafts (31). Treatment with MBCD is widely used to study phagosome formation and maturation in phagocytosis-mediated MØ defense mechanisms against intracellular bacteria. For example, in the phagocytosis of *Salmonella typhimurium* (2, 10), *Chlamydia trachomatis* (19), *Brucella spp.* (17, 38), *M. bovis* BCG (4, 5, 11) or *M. kansasii* (22), reduction of DRM integrity by MBCD treatment modifies phagosome formation, and the enhanced fusion of bacterial phagosomes with lysosomes in MBCD-treated M∅ with reduced intracellular survival of bacteria has been reported. It was shown that mycobacterial lipamide dehydrase C interacts with actin binding protein coronin-1 on the phagosomal membrane, resulting in inhibition of maturation of the phagosome to a bactericidal phagolysosome, and that this interaction is cholesterol-dependent (5).

In this study, we have investigated the contribution of M∅ membrane cholesterol to chitin phagocytosis, phagosome formation and chitin-induced Th1 adjuvant activity using MBCD-treated RAW 264.7 MØ. We found that the initial recognition and internalization of chitin particles were not significantly different between untreated and MBCD-treated MØ. However, in MBCD-treated MØ compared to untreated MØ, the initial activation of all MAPK family members was significantly accelerated and enhanced by chitin microparticles. The initial phase of MAPK phosphorylation in MBCD-treated cells was followed by significant enhancement of

TNF-α and COX-2, but not IL-10, production. Treatment with MBCD only minimally enhanced MØ activation induced by CpG-ODN, HK-BCG or HK-*Listeria monocytogenes*.

MATERIALS AND METHODS

Reagents and antibodies

Chitin powder was purchased from Sigma (St. Louis, MO) and 1 – 10 μm and >50 μm chitin particles and 1 – 10 μm chitosan (de-acetylated chitin) particles were prepared as described previously (18, 29). Soluble chitin oligosaccharide was provided by Kyowa Technos (Chiba, Japan). Latex beads (1.1 μm, polystyrene), MBCD, and arachidonic acid (AA) were purchased from Sigma. CpG-ODN (5' TCC ATG ACG TTC CTG ACG TT 3'; unmethylated) with a phosphorothioate backbone was purchased from TriLink (Sorrento Mesa, CA). The cultured bacteria of *M. bovis* BCG Tokyo 172 strain were washed, autoclaved, and lyophilized (28). *Listeria monocytogenes* 10403S serotype 1/2a was grown in brain-heart infusion broth (Difco) at 37°C. The bacteria were harvested in the logarithmic phase of growth, incubated at 60°C for 60 min, washed 3 times with cold saline. All stimulating reagents were suspended in endotoxin-free saline as 10 mg/ml stock solutions and aliquots were stored at -80°C. MBCD as a 0.5 M stock solution in endotoxin-free saline and AA as a 100 mg/ml stock solution in 100% ethanol were stored at -80˚C until use. Rabbit polyclonal antibodies (Abs) against MAPK (anti-p38, anti-ERK1/2, and anti-JNK) and dual phosphorylated MAPK (anti-p-p38, anti-p-ERK1/2, and anti-p-JNK) were purchased from Cell Signaling Technology (Beverly, MA). Rabbit polyclonal anti-COX-2 Ab was purchased from Cayman Chemicals (Ann Arbor, MI). Rat monoclonal Abs against F4/80, Mac-1, Fcγ receptor II/III (FcγR), scavenger receptor A (SR-A; 2F8), and Toll-like receptor 4 (TLR4) were purchased from BD Biosciences (San Diego, CA). Rabbit polyclonal anti-mannose receptor (MR) Ab was a gift from Dr. Philip Stahl, Washington University (St. Louis, MO).

Cholesterol depletion with MBCD

Murine MØ-like RAW 264.7 cells (American Type Culture Collection, Manassas, VA) were grown and maintained in RPMI 1640 containing 5% heat-inactivated fetal bovine serum (FBS) as described previously (18). For all experiments testing MAPK activation, MØ were incubated in serum-free RPMI 1640 at 37°C for 2 h to achieve serum starvation prior to MBCD treatment. To deplete cholesterol, MØ were incubated with 0 (saline), 1 or 5 mM MBCD at 37°C for 1 h, prior to chitin particle stimulation. Cell viability was determined by trypan blue exclusion and lactate dehydrogenase (LDH) release according to the manufacturer's instructions (Cytotoxity Colorimetric Assay Kit, Oxford Biomedical Research, Oxford, MI).

Cytometric detection of phagocytosed chitin particles and MØ surface antigens

For chitin binding and phagocytosis assays (32), 1 – 10 μm chitin particles were labeled with fluorescein isothiocyanate (FITC). Particles (10 mg) and FITC (0.1 mg) were mixed and incubated in 0.1 M $NaHCO_3$ at 22°C for 2 h. Glycine (final 1 M) was added to bind free FITC, after which labeled particles were washed and suspended in saline at 10 mg/ml. To assess cell-surface binding of chitin, MØ were incubated with 100 μg/ml FITC-chitin particles on ice for 30 min. Free particles were removed by washing three times, and cellular fluorescence was measured cytometrically (BD FACSCalibur system with CELL Quest™ acquisition plus analysis program; Becton-Dickinson Immunocytometry Systems, San Jose, CA). To confirm that MØ binding to chitin particles was not altered by FITC, an excess of unlabeled particles (1,000 μg/ml) was used to compete with FITC-chitin.

For evaluation of phagocytosis, MØ were incubated with 100 μg/ml FITC-chitin particles at 37°C for 20 or 40 min. Fluorescence of unphagocytosed FITC-chitin was quenched with 50 mM acetate-buffered saline (pH 4.5) containing 2 mg/ml trypan blue, and the fluorescence intensity of MØ with intracellular FITC-chitin particles was measured cytometrically. The presence of intracellular FITC-chitin particles was further confirmed by fluorescence microscopy (Provis AX70 Microscope with MagnaFire, Olympus, Center Valley, PA).

Expression of F4/80, Mac-1, FcγR, SR-A, TLR4, or MR on MØ was determined cytometrically as indicated previously (27).

MAPK activation

Western blot analyses of MAPK phosphorylation were performed as described previously (18). Briefly, MØ (10^6 /ml) were stimulated with each agonist or saline at 37°C for 0, 10, 20, 30, or 40 min. After cell lysis, equal amounts of cellular protein were separated by SDS-PAGE using SDS-11% polyacrylamide gel and then electroblotted onto PVDF membranes. After blocking the membrane with non-fat dry milk, proteins were stained with primary Ab (anti-p38, anti-ERK1/2, anti-JNK, anti-p-p38, anti-p-ERK1/2, or anti-p-JNK) and horseradish peroxidase-conjugated goat anti-rabbit IgG (Jackson ImmunoResearch, West Glove, PA). Stained bands were detected by chemiluminescence (ECL Western Blotting Detection Reagents, Amersham Biosciences, Piscataway, NJ) according to the manufacturer's instructions. Intensity of specific bands was quantified digitally using graphic imaging software (NIH Image 1.5).

Isolation of particle-associated cellular proteins

MBCD- or saline- treated MØ (2 x 10^6/ml) were stimulated with 100 μg/ml 1 – 10 μm chitin particles at 37°C for 10, 20, or 40 min, washed with saline, suspended in homogenization buffer (50 mM Tris-HCl, pH 7.5, 0.32 M sucrose, 10 mM NaF, 1 mM Na_3VO_4, 5 mM EDTA, 1:500 protease inhibitor cocktail [Sigma]), and homogenized by sonication (20 s). Particles were isolated from lysates by centrifugation (400 g, 4°C, 10 min) and washed 5 times with saline. Proteins associated with the particles were extracted with SDS-lysis buffer by heating at 95°C for 5 min. Total and phosphorylated p38 and ERK 1/2 as well as lysosome-associated membrane protein-1 (LAMP-1) were detected by western blotting with specific antibodies as described above. Typically, approximately 1 μg chitin-associated protein was isolated at 20 min from 10^7 saline-treated MØ. The recovery rates in this study were comparable for samples with or without MBCD treatment.

Cytokine production

MØ (5×10^5 /ml) were stimulated with agonist or saline at 37°C for 3 h (for TNF-α) and 24 h (for IL-10). TNF-α and IL-10 levels in culture supernatants were measured by specific two-site ELISA (BD Biosciences).

IL-10 mRNA expression

MØ (5×10^5 /ml) were stimulated with agonist or saline at 37°C for 6 and 24 h. Total RNA was extracted from the cells with TRizol reagent (Invitrogen, Carlsbad, CA) according to the manufacturer's instructions. IL-10 mRNA expression was examined by RT-PCR. Reverse transcription of mRNA was achieved by SuperScript™ First-Strand Synthesis System for RT-

PCR (Invitrogen) with oligo-(dT) primer according to the manufacturer's instructions. PCR primers used were IL-10 (forward: 5'-GGT TGC CAA GCC TTA TCG GA-3', reverse: 5'-ACC TGC TCC ACT GCC TTG CT-3') and GAPDH (forward: 5'-TTC ACC ACC ATG GAG AAG GC-3', reverse: 5'-GGC ATG GAC TGT GGT CAT GA-3'). PCR products (15 μl) were electrophoresed on 2% agarose gel. After ethidium bromide staining, PCR products were visualized by UV illumination.

COX-2 production and PGE_2 release

MØ (5×10^5 /ml) were stimulated with each agonist or saline at 37°C for 2 h. COX-2 in cell lysates was analyzed by Western blotting using anti-COX-2, as described previously (18).

For PGE_2 release, cells were further incubated in serum free RPMI 1640 with 1 μg/ml AA or saline at 37°C for an additional 2 h. Culture supernatants were harvested and stored at -80ºC. PGE_2 levels were assayed by ELISA (Cayman Chemicals) (18).

Cellular cholesterol level

Cholesterol was extracted from cell pellets (10^6 cells) with methanol/chloroform (2:1), followed by addition of an equal volume of chloroform/water (1:1). Cholesterol was recovered from the chloroform layer by lyophilization. Extracted lipids were dissolved in the buffer for Cholesterol E test (Wako Bioproducts, Richmond, VA) and cholesterol in the extract was determined by enzymatic colorimetric assay, according to the manufacturer's instructions. Cellular protein was measured, as described previously (18) and cholesterol levels were normalized to the protein levels. Normalized cholesterol levels of saline-treated MØ were considered as 100%.

Endotoxin removal

Endotoxin was removed from soluble materials for culture by filtration and sterilization through a 0.22-μm Zetapore membrane (AMF-Cuno; Cuno, Meriden, CT) (21). Chitin particles and heat-killed bacteria were suspended in and washed with endotoxin-free saline. The final preparations were monitored for endotoxin by the *Limulus* amebocyte assay (Sigma) (26). No endotoxin was detected in suspensions of chitin particles, HK-BCG, or HK-*L. monocytogenes*.

Statistics

Differences between mean values were analyzed by the Wilcoxan Rank Sum Test or the Mann-Whitney. $P < 0.05$ is considered statistically significant.

RESULTS

Cholesterol depletion of MØ does not significantly alter initial phagocytosis of chitin particles.

To investigate the effects of cholesterol depletion on MØ viability, RAW 264.7 cells were treated with 1, 5, 7.5, 10, 15, or 20 mM MBCD. Treatment of MØ with 5 mM MBCD, which has been used to inhibit phagocytosis of intracellular bacteria (17, 38), in the presence or absence of 5% heat-inactivated FBS reduced cellular cholesterol levels to 40 – 45% of that present prior to treatment (Fig. 1A). Treatment of MØ with 5 mM or less MBCD did not reduce cell viability at 24 h (Fig. 1B).

We determined the effect of cholesterol depletion on expression of the selected MØ surface antigens F4/80, Mac-1, FcγR, SR-A, TLR4, and MR. As shown in Table 1, these antigens were constitutively expressed, respectively, by 61, 85, 71, 85, 80, and 86% of RAW264.7 cells. The expression of F4/80 was slightly increased (Table 1; 69% of MØ), whereas Mac-1, FcγR, and SR-A were slightly reduced (81, 65, and 81% of MØ, respectively) by treatment with 5 mM MBCD. The expression of TLR4 and MR were not altered by MBCD. Levels of mean fluorescence intensity also supported the effects of MBCD on the M∅ antigens (Table 1). Therefore, MBCD at 5 mM or less was used for further experiments. All studies of chitin stimulation in the presence of MBCD were terminated within 6 h.

We also determined whether cholesterol depletion modifies MØ binding and internalization of FITC-chitin microparticles. As shown in Figure 2A, 80% of saline-treated MØ bound to FITC-

chitin particles, which was not significantly altered by MBCD treatment. This binding was completely inhibited in the presence of non-labeled chitin particles, but not latex beads (data not shown). Internalization of FITC-chitin particles at 37ºC was analyzed following quenching of unphagocytosed FITC-chitin. As shown in Figure 2B, the magnitude of phagocytosis is similar for MBCD- and saline- treated MØ at 20 min (12 and 12%, respectively). Saline-treated MØ may have internalized more particles than MBCD-treated MØ at 20 min, since the peak fluorescence intensity was slightly reduced by MBCD treatment (Fig. 2B). However, phagocytosis at 40 min was significantly reduced in MBCD-treated MØ (33 ± 2.8 and 21 ± 0.9% [mean ± SEM, n=3, $p<0.01$] for saline- and MBCD- treated MØ, respectively).

Other particles including HK-BCG, HK-*L. monocytogenes*, 1 – 10 μm chitosan and 1.1 μm latex beads were phagocytosed by MBCD-treated or untreated MØ without changing phagocytic capacities within 40 min after particle stimuli (data not shown).

Chitin -induced MAPK phosphorylation is accelerated and enhanced by cholesterol depletion.

We demonstrated that when MØ phagocytosed chitin particles, MØ MAPK families including p38, ERK1/2 and JNK were phosphorylated (18). Treatment of MØ with MBCD alone at 1 or 5 mM resulted in no significant phosphorylation of p38, ERK1/2 or JNK during the experimental period (Fig. 3A). As shown in Figure 3A and B, at 20 min after chitin particle stimulation, the levels of phosphorylated p38 and ERK1/2 in MBCD-treated cells were markedly increased compared with those in saline-treated MØ. At 40 min, the magnitudes of ERK1/2 activation in MBCD-treated MØ decreased but for p-p38 were still higher than for saline-treated MØ

phagocytosing chitin particles (Fig. 3B). The enhanced phosphorylation of each MAPK was greater at 5 mM than at 1 mM MBCD (Fig. 3A). We also found that accelerated and enhanced phosphorylation of JNK at kinetics similar to that of p-p38 in MBCD-treated M∅ (data not shown).

The effects of MBCD were relatively selective for chitin microparticles, since MAPK activation by other agonists, CpG-ODN, HK-BCG, and HK-*L. monocytogenes* was relatively insensitive to the treatment with MBCD (Fig. 4).

We have previously found that cellular activation in response to chitin occurs specifically with phagocytosable particles, but not soluble chitin oligosaccharide, non-phagocytosable chitin particles (>50 μm), 1 – 10 μm chitosan particles, or 1.1 μm latex beads (18). We observed that for other than phagocytosable chitin microparticles, there was no effect of MBCD-treatment on M∅ activation (Fig. 5).

Phosphorylation of p38 and ERK1/2 associated with intracellular chitin particles is accelerated and enhanced by cholesterol depletion.

We next determined the extent of phosphorylation of MAPK associated with intracellular chitin particles in MBCD-treated and saline-treated M∅. Cellular proteins associated with chitin particles were isolated from MBCD- and saline- treated cells 10, 20 and 40 min after phagocytosis of chitin particles. Following fusion with late endosomes/lysosomes, matured phagosomes express LAMP-1 (24). The levels of LAMP-1 in whole cell lysates were comparable for saline- and MBCD- treated cells (Fig. 6A). MAPKs p38 and ERK 1/2 and the

respective phosphorylated forms were detected in the particle-associated fractions at 10, 20 and 40 min (Fig. 6A). The ratios of band intensity for the phosphorylated relative to the total MAPK are shown in Figure 6B. The relative amounts of chitin-associated phoshorylated MAPK were greater in the MBCD- than in saline- treated cells. Phosphorylated JNK was not detected in the particle-associated fraction (data not shown).

Cholesterol depletion enhances chitin-induced TNF-α production and COX-2-mediated PGE_2 synthesis

Although treatment with MBCD alone did not result in observable MAPK activation, 5 mM MBCD enhanced slightly but significantly TNF-α production. Treatment with 1 mM MBCD resulted in 3- and 1.8- fold increases in TNF-α production in response to 20 and 100 μg/ml chitin particles, respectively. There was similar enhancement for MØ treated with 5 mM MBCD (Fig. 7A). In response to 0.2 or 1.0 μg/ml CpG-ODN, TNF-α production was significantly increased for MØ treated with 5 mM, but not 1 mM, MBCD (Fig. 7A). However, since 5 mM MBCD alone enhanced the base line of TNF-α production, the effect on CpD-ODN-induced TNF-α was minimal. Neither HK-BCG nor HK-*L. monocytogenesis* induced TNF-α production was affected by cholesterol depletion (Fig. 7A).

COX-2 expression was induced by treatment with 5 mM MBCD alone, and was further enhanced by 100 μg/ml chitin particles (Fig. 7B). Following treatment with 1 mM MBCD, increased chitin particle-induced COX-2 expression is associated with increased PGE_2 release. As shown in Figure 7C, chitin particle-activated MØ released 233 ± 11 and 506 ± 52 pg/ml PGE_2 in the absence and presence of 1 mM MBCD, respectively. However, for MØ were treated with

5 mM MBCD the release of PGE_2 was not different from that of MØ treated with saline despite the increased COX-2 expression (Figs. 7B, 7C). After treatment with 5 mM MBCD, nuclear envelope localization and COX-2 enzyme activity were intact (data not shown). Therefore, additional factors that may include phospholipase A2, PGE synthases and/or the assembly of these enzymes at membrane sites may be impaired by cholesterol depletion by 5 mM MBCD. CpG-ODN also induces COX-2-mediated PGE_2 biosynthesis (18). The treatment with 1 mM MBCD did not enhance CpG-ODN-induced COX-2 expression (Fig. 7B) or PGE_2 release (data not shown).

Effects of cholesterol depletion on chitin-induced IL-10 production

Despite the release of TNF-α and PGE_2, which are both endogenous inducers of IL-10 (7, 30, 33), we found previously that chitin particles do not induce IL-10 expression by MØ at 24 h (18), nor was IL-10 mRNA detected (Fig. 8). In contrast, CpG-ODN-induced expression of IL-10 was significantly increased at 24 h, as described previously (18) with mRNA synthesis observed (Fig. 8). We further determined the effect of cellular cholesterol depletion on chitin particle-induced IL-10 expression. As shown in Figure 8, MBCD treatment prior to exposure to chitin particles did not result in IL-10 mRNA expression at 6 h. CpG-ODN-induced IL-10 mRNA was not increased by MBCD treatment (Fig. 8). Taken together, our results indicate that following cholesterol depletion, the Th1 adjuvant chitin does not induce IL-10 production, despite effects on MAPK phosphorylation, TNF-α production and PGE_2 biosynthesis.

DISCUSSION

Chitin microparticles have been considered a unique and clinically useful Th1 adjuvant, since administration of chitin microparticles in mouse models of asthma and mycobacterial infections promotes MØ activation leading to the down-regulation of allergic responses and the enhancement of host immunity against mycobacteria, respectively (25, 28). Our previous (18, 29) and present studies clearly indicate that both recognition and phagocytic entry of chitin microparticles are required for MØ activation characterized by MAPK phosphorylation, Th1 cytokine production and COX-2-mediated PGE_2 biosynthesis. The depletion of cholesterol in the plasma membrane results in only minimal alteration in the recognition and internalization of chitin particles, HK-BCG or HK-*L. monocytogenes* within 20 min after particle stimulation (Fig. 2). However, the rate and extent of chitin particle-induced MAPK phosphorylation are accelerated and enhanced, respectively, for MBCD-treated MØ compared to saline-treated MØ (Fig. 3). This is also detected in phagosomes including chitin microparticles (Fig. 6). In contrast, up-modulation of MAPK phosphorylation following depletion of cholesterol was only slight in stimulation with HK-BCG, HK-*L. monocytogenes* or CpG-ODN (Fig. 4). These results indicate that phosphorylation of MAPKs in the MØ response to chitin microparticles, but not to HK-BCG, HK-*L. monocytogenes* or CpG-ODN is enhanced by depletion of membrane cholesterol.

Our previous studies with MØ (18, 26, 29) clearly indicate that phagocytosis of chitin microparticles (1 – 10 μm), but not a soluble form of chitin or >50 μm chitin particles, promotes MAPK activation and Th1 responses. The present study further indicates that, in contrast to

results for phagocytosable chitin microparticles (1 – 10 μm), MAPK activation in response to >50 μm chitin particles, soluble chitin, 1 – 10 μm chitosan particles, or 1.1 μm latex beads is not altered by MBCD treatment of MØ. Thus, requirements for recognition and response to chitin preparations and latex beads are not qualitatively altered by MBCD-treatment. GlcNAc residues are recognized by mannose-type C-type lectin-like receptors (CLR) including MR, endo-180 and dendritic cell-specific ICAM-grabbing non-integrin (DC-SIGN), which is located in the DRM of dendritic cells (16, 23). Although receptor(s), other than MR, that contribute to phagocytosis of chitin particles, have not been completely identified, MBCD treatment does not change the capacity of RAW264.7 cells for chitin binding or phagocytosis at 20 min (Fig. 2).

It is likely that cellular signals for both MAPK phosphatase activation and attenuation are also induced by chitin. Our results are consistent with either enhanced activity of MAPK kinases (MAPKKs) or the inhibition of MAPK phosphatase (MKP) activity following disruption of the integrity of DRM by MBCD. Previous studies suggest that DRM-associated regulation of cellular signaling may depend on caveolin-, oxysterol-binding protein (OSBP)-, and phosphatidylinositol-3 kinase (PI3K)- mediated mechanisms (3, 8, 9, 12, 20, 36, 37). Further studies to determine whether these molecules are involved in chitin-induced M∅ activation are underway.

Another finding is that depletion of MØ cholesterol results in significant enhancement of chitin microparticle-induced MØ production of TNF-α, a Th1 cytokine (Fig. 7). In MØ treated with 1 mM MBCD, TNF-α production and COX-2-mediated PGE_2 biosynthesis are significantly increased. In response to chitin particles, the production of PGE_2 has a biphasic dependence on

cellular cholesterol levels. Following treatment with 1 mM MBCD and chitin particle stimulation, the increase in PGE_2 correlates with the increase in COX-2 expression. However, chitin particles do not induce IL-10 mRNA or IL-10, in agreement with our previous report (18), despite the fact that chitin particles induce PGE_2 and TNF-α that potentially promote IL-10 production (7, 30, 33). This study provides further support for a MAPK-independent mechanism for stimulation of IL-10 production.

In addition to the present results of TNFα and IL-10, RAW264.7 cells produced detectable levels of IL-1β, IL-6 and GM-CSF in response to chitin microparticles (data not shown). RAW264.7 cells that are stimulated with LPS result in phosphorylation of p38 and ERK1/2 followed by these cytokine productions (15, 34). Our preliminary studies indicated that these chitin particle-induced cytokine productions were enhanced by MBCD-treated cells (data not shown). Further studies are required to determine whether other cytokine productions which are dependent on or independent of MAPK phosphorylation are enhanced under membrane cholesterol depletion.

In contrast to stimulation by chitin microparticles, MAPK activation in response to HK-BCG and HK-*L. monocytogenes* is relatively insensitive to cholesterol depletion. These microbes are recognized by multiple receptors including Toll-like receptors and scavenger receptors (1, 16). We have also observed that inhibition of phagocytosis of these microbes by cytochalasin D does not prevent MAPK activation and Th1 cytokine production (data not shown). Solublized components of HK-BCG, prepared by filtration of sonicated HK-BCG solution through a 0.22 μm Millipore membrane, induced TNFα production and COX-2 expression (data not shown). These results suggest that phagocytic entry and phagosome formation are not required for

MAPK activation by the HK-bacteria. Furthermore, CpG-ODN, a soluble component of bacteria, induces MAPK activation and Th1 cytokine production in a TLR9-mediated manner which does not require actin polymerization (13, 18) and is not altered by depletion of membrane cholesterol (Fig. 4). It is therefore likely that MØ activation signals derived from phagocytic entry and phagosome formation are more sensitive to the cholesterol depletion than recognition of microparticles.

In conclusion, although the early phase of phagocytosis of chitin microparticles is comparable for untreated MØ and MØ depleted of cholesterol by MBCD, MAPK activation and Th1 cytokine production in response to chitin is markedly enhanced in MBCD-treated MØ. Our results suggest differential membrane structural requirements for MAPK activation, and cytokine or PGE_2 production compared to binding and phagocytosis of chitin particles. IL-10 is not produced in response to chitin and this is not altered by cholesterol depletion. Although cholesterol depletion does not significantly alter initial stages of chitin phagocytosis, or MAPK activation and Th1 cytokine production by HK-BCG or HK-*L. monocytogenes*, membrane structures integrated by cholesterol appear to be important for the normal regulation of chitin-induced MØ MAPK activation, probably reflecting phagocytic entry and phagosome formation as well as cellular recognition by different surface receptors.

ACKNOWLEDGMENTS

This work was supported by NIH RO1 HL7171, DOD DAMD 17-03-1-0004 and the Charles E. Schmidt Biomedical Foundation, and funds from Florida Atlantic University.

REFERENCES

1. **Akira S**. Toll-like receptor signaling. *J Biol Chem* 278: 38105-38108, 2003.

2. **Catron DM, Sylvester MD, Lange Y, Kadekoppala M, Jones BD, Monack DM, Falkow S, and Haldar K**. The Salmonella-containing vacuole is a major site of intracellular cholesterol accumulation and recruits the GPI-anchored protein CD55. *Cell Microbiol* 4: 315-328, 2002.

3. **Cho KA, Ryu SJ, Park JS, Jang IS, Ahn JS, Kim KT, and Park SC**. Senescent phenotype can be reversed by reduction of caveolin status. *J Biol Chem* 278: 27789-27795, 2003.

4. **de Chastellier C, and Thilo L**. Cholesterol depletion in Mycobacterium avium-infected macrophages overcomes the block in phagosome maturation and leads to the reversible sequestration of viable mycobacteria in phagolysosome-derived autophagic vacuoles. *Cell Microbiol* 8: 242-256, 2006.

5. **Deghmane AE, Soulhine H, Bach H, Sendide K, Itoh S, Tam A, Noubir S, Talal A, Lo R, Toyoshima S, Av-Gay Y, and Hmama Z**. Lipoamide dehydrogenase mediates retention of coronin-1 on BCG vacuoles, leading to arrest in phagosome maturation. *J Cell Sci* 120: 2796-2806, 2007.

6. **Desjardins M, and Griffiths G**. Phagocytosis: latex leads the way. *Curr Opin Cell Biol* 15: 498-503, 2003.

7. **Foey AD, Parry SL, Williams LM, Feldmann M, Foxwell BM, and Brennan FM**. Regulation of monocyte IL-10 synthesis by endogenous IL-1 and TNF-alpha: role of the p38 and p42/44 mitogen-activated protein kinases. *J Immunol* 160: 920-928, 1998.

8. **Fukao T, Tanabe M, Terauchi Y, Ota T, Matsuda S, Asano T, Kadowaki T, Takeuchi T, and Koyasu S**. PI3K-mediated negative feedback regulation of IL-12 production in DCs. *Nat Immunol* 3: 875-881, 2002.

9. **Furuchi T, and Anderson RG**. Cholesterol depletion of caveolae causes hyperactivation of extracellular signal-related kinase (ERK). *J Biol Chem* 273: 21099-21104, 1998.

10. **Garner MJ, Hayward RD, and Koronakis V**. The Salmonella pathogenicity island 1 secretion system directs cellular cholesterol redistribution during mammalian cell entry and intracellular trafficking. *Cell Microbiol* 4: 153-165, 2002.

11. **Gatfield J, and Pieters J**. Essential role for cholesterol in entry of mycobacteria into macrophages. *Science* 288: 1647-1650, 2000.

12. **Guha M, and Mackman N**. The phosphatidylinositol 3-kinase-Akt pathway limits lipopolysaccharide activation of signaling pathways and expression of inflammatory mediators in human monocytic cells. *J Biol Chem* 277: 32124-32132, 2002.

13. **Hacker H, Redecke V, Blagoev B, Kratchmarova I, Hsu LC, Wang GG, Kamps MP, Raz E, Wagner H, Hacker G, Mann M, and Karin M**. Specificity in Toll-like receptor signalling through distinct effector functions of TRAF3 and TRAF6. *Nature* 439: 204-207, 2006.

14. **Henson PM, Bratton DL, and Fadok VA**. Apoptotic cell removal. *Curr Biol* 11: R795-805, 2001.

15. **Kim K, Duramad O, Qin XF, and Su B**. MEKK3 is essential for lipopolysaccharide-induced interleukin-6 and granulocyte-macrophage colony-stimulating factor production in macrophages. *Immunology* 120: 242-250, 2007.

16. **McGreal EP, Miller JL, and Gordon S**. Ligand recognition by antigen-presenting cell C-type lectin receptors. *Curr Opin Immunol* 17: 18-24, 2005.

17. **Naroeni A, and Porte F**. Role of cholesterol and the ganglioside GM(1) in entry and short-term survival of Brucella suis in murine macrophages. *Infect Immun* 70: 1640-1644, 2002.

18. **Nishiyama A, Tsuji S, Yamashita M, Henriksen RA, Myrvik QN, and Shibata Y**. Phagocytosis of N-acetyl-D-glucosamine particles, a Th1 adjuvant, by RAW 264.7 cells results in MAPK activation and TNF-alpha, but not IL-10, production. *Cell Immunol* 239: 103-112, 2006.

19. **Norkin LC, Wolfrom SA, and Stuart ES**. Association of caveolin with Chlamydia trachomatis inclusions at early and late stages of infection. *Exp Cell Res* 266: 229-238, 2001.

20. **Park WY, Park JS, Cho KA, Kim DI, Ko YG, Seo JS, and Park SC**. Up-regulation of caveolin attenuates epidermal growth factor signaling in senescent cells. *J Biol Chem* 275: 20847-20852, 2000.

21. **Petsch D, Beeskow TC, Anspach FB, and Deckwer WD**. Membrane adsorbers for selective removal of bacterial endotoxin. *J Chromatogr B Biomed Sci Appl* 693: 79-91, 1997.

22. **Peyron P, Bordier C, N'Diaye EN, and Maridonneau-Parini I**. Nonopsonic phagocytosis of Mycobacterium kansasii by human neutrophils depends on cholesterol and is mediated by CR3 associated with glycosylphosphatidylinositol-anchored proteins. *J Immunol* 165: 5186-5191, 2000.

23. **Pontow SE, Kery V, and Stahl PD**. Mannose receptor. *Int Rev Cytol* 137B: 221-244, 1992.

24. **Scott CC, Botelho RJ, and Grinstein S**. Phagosome maturation: a few bugs in the system. *J Membr Biol* 193: 137-152, 2003.

25. **Shibata Y, Foster LA, Bradfield JF, and Myrvik QN**. Oral administration of chitin down-regulates serum IgE levels and lung eosinophilia in the allergic mouse. *J Immunol* 164: 1314-1321, 2000.

26. **Shibata Y, Foster LA, Kurimoto M, Okamura H, Nakamura RM, Kawajiri K, Justice JP, Van Scott MR, Myrvik QN, and Metzger WJ**. Immunoregulatory roles of IL-10 in innate immunity: IL-10 inhibits macrophage production of IFN-gamma-inducing factors but enhances NK cell production of IFN-gamma. *J Immunol* 161: 4283-4288, 1998.

27. **Shibata Y, Gabbard J, Yamashita M, Tsuji S, Smith M, Nishiyama A, Henriksen RA, and Myrvik QN**. Heat-killed BCG induces biphasic cyclooxygenase 2+ splenic macrophage formation--role of IL-10 and bone marrow precursors. *J Leukoc Biol* 80: 590-598, 2006.

28. **Shibata Y, Honda I, Justice JP, Van Scott MR, Nakamura RM, and Myrvik QN**. Th1 adjuvant N-acetyl-D-glucosamine polymer up-regulates Th1 immunity but down-regulates Th2 immunity against a mycobacterial protein (MPB-59) in interleukin-10-knockout and wild-type mice. *Infect Immun* 69: 6123-6130, 2001.

29. **Shibata Y, Metzger WJ, and Myrvik QN**. Chitin particle-induced cell-mediated immunity is inhibited by soluble mannan: mannose receptor-mediated phagocytosis initiates IL-12 production. *J Immunol* 159: 2462-2467, 1997.

30. **Shinomiya S, Naraba H, Ueno A, Utsunomiya I, Maruyama T, Ohuchida S, Ushikubi F, Yuki K, Narumiya S, Sugimoto Y, Ichikawa A, and Oh-ishi S**. Regulation of TNFalpha and interleukin-10 production by prostaglandins I(2) and E(2): studies with prostaglandin receptor-deficient mice and prostaglandin E-receptor subtype-selective synthetic agonists. *Biochem Pharmacol* 61: 1153-1160, 2001.

31. **Simons K, and Ikonen E**. Functional rafts in cell membranes. *Nature* 387: 569-572, 1997.

32. **Takizawa F, Tsuji S, and Nagasawa S**. Enhancement of macrophage phagocytosis upon iC3b deposition on apoptotic cells. *FEBS Lett* 397: 269-272, 1996.

33. **Treffkorn L, Scheibe R, Maruyama T, and Dieter P**. PGE2 exerts its effect on the LPS-induced release of TNF-alpha, ET-1, IL-1alpha, IL-6 and IL-10 via the EP2 and EP4 receptor in rat liver macrophages. *Prostaglandins Other Lipid Mediat* 74: 113-123, 2004.

34. **Tudhope SJ, Finney-Hayward TK, Nicholson AG, Mayer RJ, Barnette MS, Barnes PJ, and Donnelly LE**. Different mitogen-activated protein kinase-dependent cytokine responses in cells of the monocyte lineage. *J Pharmacol Exp Ther* 324: 306-312, 2008.

35. **Underhill DM, and Ozinsky A**. Phagocytosis of microbes: complexity in action. *Annu Rev Immunol* 20: 825-852, 2002.

36. **Wang PY, Liu P, Weng J, Sontag E, and Anderson RG**. A cholesterol-regulated PP2A/HePTP complex with dual specificity ERK1/2 phosphatase activity. *Embo J* 22: 2658-2667, 2003.

37. **Wang PY, Weng J, and Anderson RG**. OSBP is a cholesterol-regulated scaffolding protein in control of ERK 1/2 activation. *Science* 307: 1472-1476, 2005.

38. **Watarai M, Makino S, Fujii Y, Okamoto K, and Shirahata T**. Modulation of Brucella-induced macropinocytosis by lipid rafts mediates intracellular replication. *Cell Microbiol* 4: 341-355, 2002.

39. **Yeung T, and Grinstein S**. Lipid signaling and the modulation of surface charge during phagocytosis. *Immunol Rev* 219: 17-36, 2007.

Footnotes

1. Abbreviations used in this paper: MØ, macrophages; GlcNAc, *N*-acetyl-D-glucosamine; COX-2, cyclooxygenase 2; PGE_2, prostaglandin E_2; MBCD, methyl-β-cyclodextrin; DRM, detergent-resistant cholesterol-rich microdomains; ODN, oligonucleotides; CLR, C type lectin-like receptor; MR, mannose receptor; FcγR, Fcγ receptor II/III; SR-A, scavenger receptor A; TLR, Toll-like receptors; FITC, fluorescein isothiocyanate; EGFR, epidermal growth factor receptor; MAPKK, MAPK kinase; MKP, MAPK phosphatase

Legends for Figures

Fig. 1. The effects of MBCD treatment of RAW264.7 cells on cellular cholesterol level and cell viability. RAW264.7 cells were suspended in serum-free RPMI1640 or RPMI1640 containing 5% FBS at $1x10^6$ /ml and treated with MBCD at the indicated concentrations or saline at 37 ˚C. *A.* After 1-hr incubation at 5 mM MBCD, cellular cholesterol and protein were extracted. Cellular cholesterol and protein levels were measured by enzymatic colorimetric assay and BCA reagent, respectively. Cellular cholesterol level was normalized by cellular protein level. Normalized cholesterol levels of saline-treated MØ are considered as 100%. Mean ± SEM, n=3; #, $p < 0.0001$, compared to saline-treated MØ. *B.* After 24-hr incubation, viability of MØ was determined by LDH release assay of culture supernatants. Viability of saline-treated MØ was considered as 100%. The data shown are representative of three independent experiments. Mean ± SEM, n=3.

Fig. 2. The effects of MBCD on MØ cell membrane. M∅ were treated with saline or 5 mM MBCD. *A*. MØ binding to FITC chitin particles. MBCD- and saline- treated MØ were incubated with FITC-chitin particles on ice for 30 min. After washing, total fluorescence of MØ associated with FITC-chitin was monitored cytometrically. Cells in M1 gate were considered positive for chitin binding. Solid line with white background, saline treatment and FITC-chitin; solid line with gray background, MBCD treatment and FITC-chitin; dashed line with white background, saline treatment alone; dashed line with black background, MBCD treatment alone. *B*. MØ phagocytosis of FITC-chitin particles for 20 and 40 min. After quenching unphagocytosed FITC chitin particles, intracellular fluorescence at 20 and 40 min was monitored.

Cells in M1 gate were considered phagocytic cells. Open background, no particles; gray background, FITC-chitin. The data shown are representative of three independent experiments.

Fig. 3. Treatment of MØ with MBCD enhances chitin particle-induced phosphorylation of p38, ERK1/2, and JNK. *A.* Western blots showing phoshorylated MAPK. MØ were pre-treated with MBCD at the indicated concentrations at 37°C for 1 h and then stimulated with chitin particles or saline at 37°C for 0, 10, 20, 30 or 40 min. Equal amounts of cellular protein were analyzed by SDS-PAGE and Western blotting. *B.* Intensities of MAPK bands detected in chitin- treated MØ were quantified digitally and the fraction of phosphorylated MAPK was normalized by the corresponding total MAPK band. ■, treated with 0 mM MBCD (saline); □, treated with 5 mM MBCD. The data shown are representative of three independent experiments.

Fig. 4. MAPK phosphorylation induced by CpG-ODN, HK-BCG and HK-*L. monocytogenes* in MBCD-treated MØ. *A*. MBCD- and saline- treated MØ were stimulated with 5 μg/ml CpG-ODN, 100 μg/ml HK-BCG, or 100 μg/ml HK-*L. monocytogenes* at 37°C for 0, 10, 20, 30 or 40 min. Other procedures were identical to those in Figure 3*A*. The data shown are representative of three independent experiments.

Fig. 5. Effects of MBCD on MAPK activation induced by control agonists. MBCD- and saline-treated MØ were stimulated with 100 μg/ml 1 – 10 μm chitin particles, 100 μg/ml soluble chitin oligosaccharide, 100 μg/ml >50 μm chitin particles, 100 μg/ml 1 – 10 μm chitosan particles, or 100 μg/ml 1.1 μm latex beads at 37°C for 0, 10, 20, 30 and 40 min. Experiments were

performed as described for Fig. 3A. The data shown are representative of three independent experiments.

Fig. 6. Phagosomal localization of MAPK proteins. MBCD- and saline- treated MØ were stimulated with 100 μg/ml 1 – 10 μm chitin particles at 37°C for 10, 20 or 40 min. Chitin particle-associated proteins were isolated and extracted as described in MATERIALS AND METHODS. Particle-associated proteins derived from 2×10^6 MØ as well as whole cell proteins were separated on SDS-11% polyacrylamide gel and electroblotted to PVDF membrane (*A*). Intensities of p38 and ERK 1/2 bands detected in phagosomal proteins (*B*) were quantified digitally using graphic imaging software (NIH Image 1.5). Ratios of the intensity of phosphorylated to total MAPK bands are shown. ■, saline-treated; □, MBCD-treated. The data shown are representative of two independent experiments.

Fig. 7. The effect of MBCD on chitin particle-induced TNF-α production, COX-2 expression, and PGE_2 release. MBCD- and saline-treated MØ were stimulated with indicated doses of agonists. *A*. The levels of TNF-α in culture supernatants 3 h after agonist stimulation were measured by ELISA. Mean ± SEM, n=3; *, $p < 0.05$; #, $p < 0.01$, compared to TNF-α induced in saline-treated cells stimulated with same dose of agonist. *B*. COX-2 levels in the cell lysate 2 h after agonist stimulation were detected by Western blotting. *C*. MØ stimulated with chitin particles (■) or saline (□) for 2 h were further elicited with 1 μg/ml AA for additional 2 hr. The levels of PGE_2 in culture supernatants were measured by ELISA. Mean ± SEM, n=3. #, $p < 0.01$, compared to PGE_2 induced in absence of MBCD and stimulated with the same agonist. The data shown are representative of three independent experiments.

Fig. 8. The effect of MBCD on IL-10 production by chitin particle-stimulated MØ. MØ treated with MBCD at 0 (saline), 1 and 5 mM were stimulated with chitin particles, CpG-ODN, or saline at 37°C for 6 h. After extraction of total RNA, RT-PCR was performed as described in MATERIALS AND METHODS. Levels of IL-10 and GAPDH mRNA are shown. These data are representative of three independent experiments.

TABLE 1. The effects of MBCD on surface expression of MØ antigens.

Antigen	% positive cells in M1 [b]		MFI[c]	
	0 mM (saline)	5 mM MBCD[a]	0 mM (saline)	5 mM MBCD[a]
F4/80	61	69	15	17
Mac-1	85	81	47	36
FcγR	71	65	17	14
SR-A	85	81	41	32
TLR4	80	79	24	23
MR	86	86	73	73

[a] MØ were treated with saline or 5 mM MBCD.

[b] Data shown are percentages of positive cells reacting to primary antibodies listed, from which percentage of cells stained with secondary Ab alone has been subtracted.

[c] Data shown were mean fluorescent intensities (MFI). The 2nd antibody controls of 0 and 5 mM MBCD treatments were both 7.0.

The data shown are representative of three independent experiments.

Fig. 1

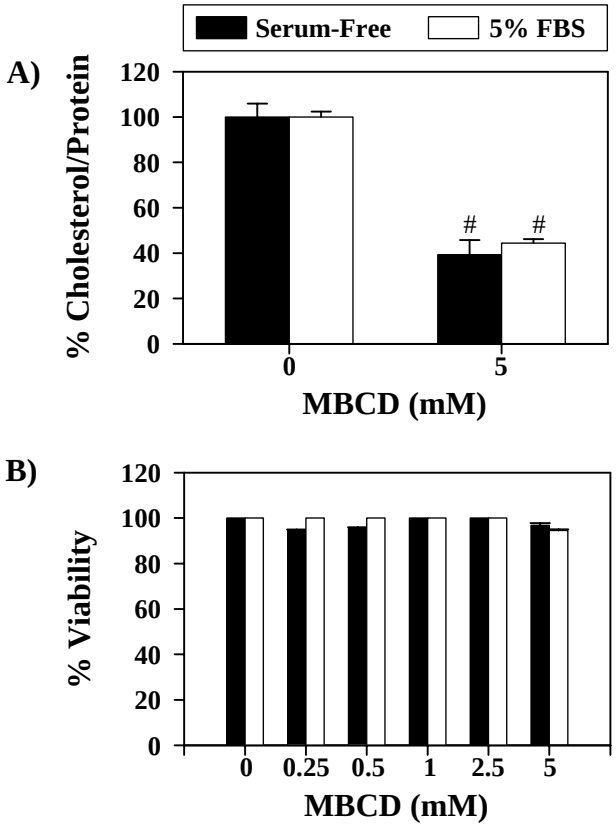
Serum-Free
5% FBS
A)
% Cholesterol/Protein
120
100
80
60
40
20
0
#
#
0
5
MBCD (mM)
B)
% Viability
120
100
80
60
40
20
0
0
0.25
0.5
1
2.5
5
MBCD (mM)

Fig. 2

(A)

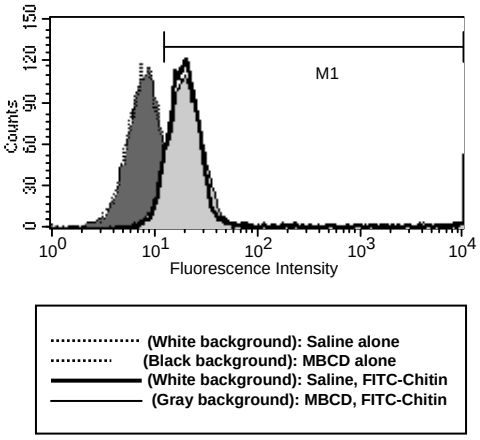
M1
Counts
Fluorescence Intensity
(White background): Saline alone
(Black background): MBCD alone
(White background): Saline, FITC-Chitin
(Gray background): MBCD, FITC-Chitin

(B)

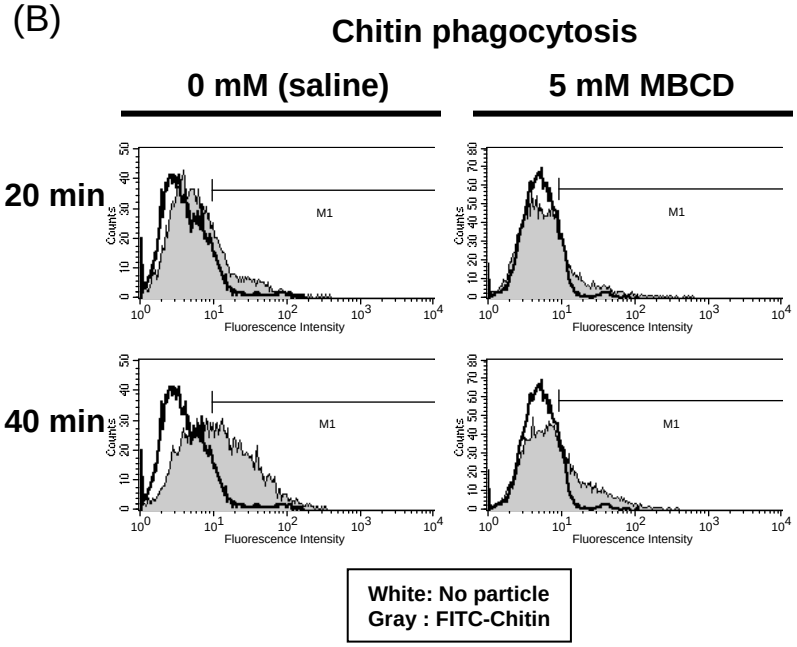
Chitin phagocytosis
0 mM (saline)
5 mM MBCD
20 min
40 min
M1
Counts
Fluorescence Intensity
White: No particle
Gray : FITC-Chitin

Fig. 3

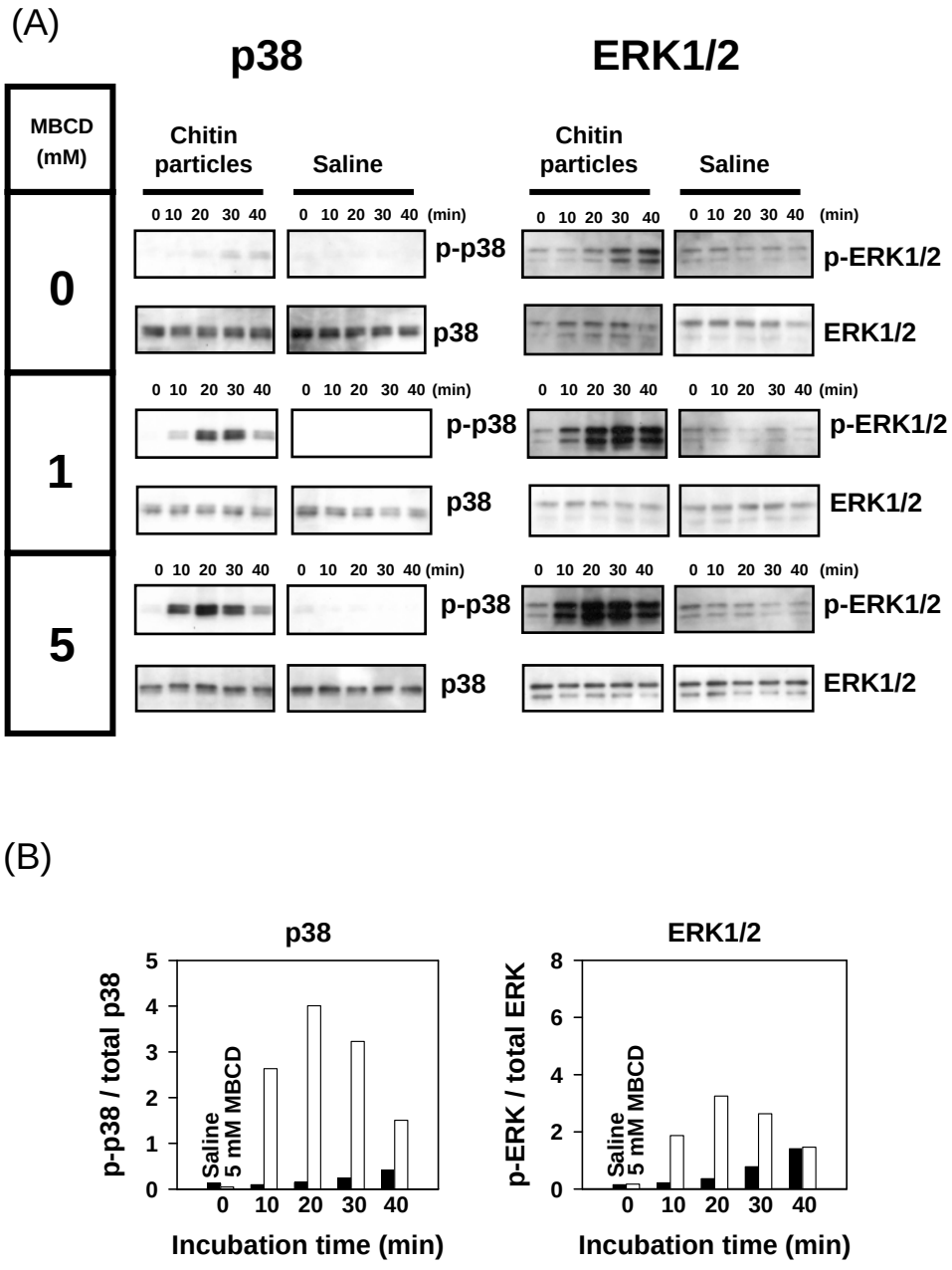
(A)
p38
ERK1/2
MBCD (mM)
Chitin particles
Saline
0 10 20 30 40 (min)
p-p38
p38
p-ERK1/2
ERK1/2
0
1
5
(B)
p38
ERK1/2
p-p38 / total p38
p-ERK / total ERK
Saline
5 mM MBCD
Incubation time (min)

Fig. 4

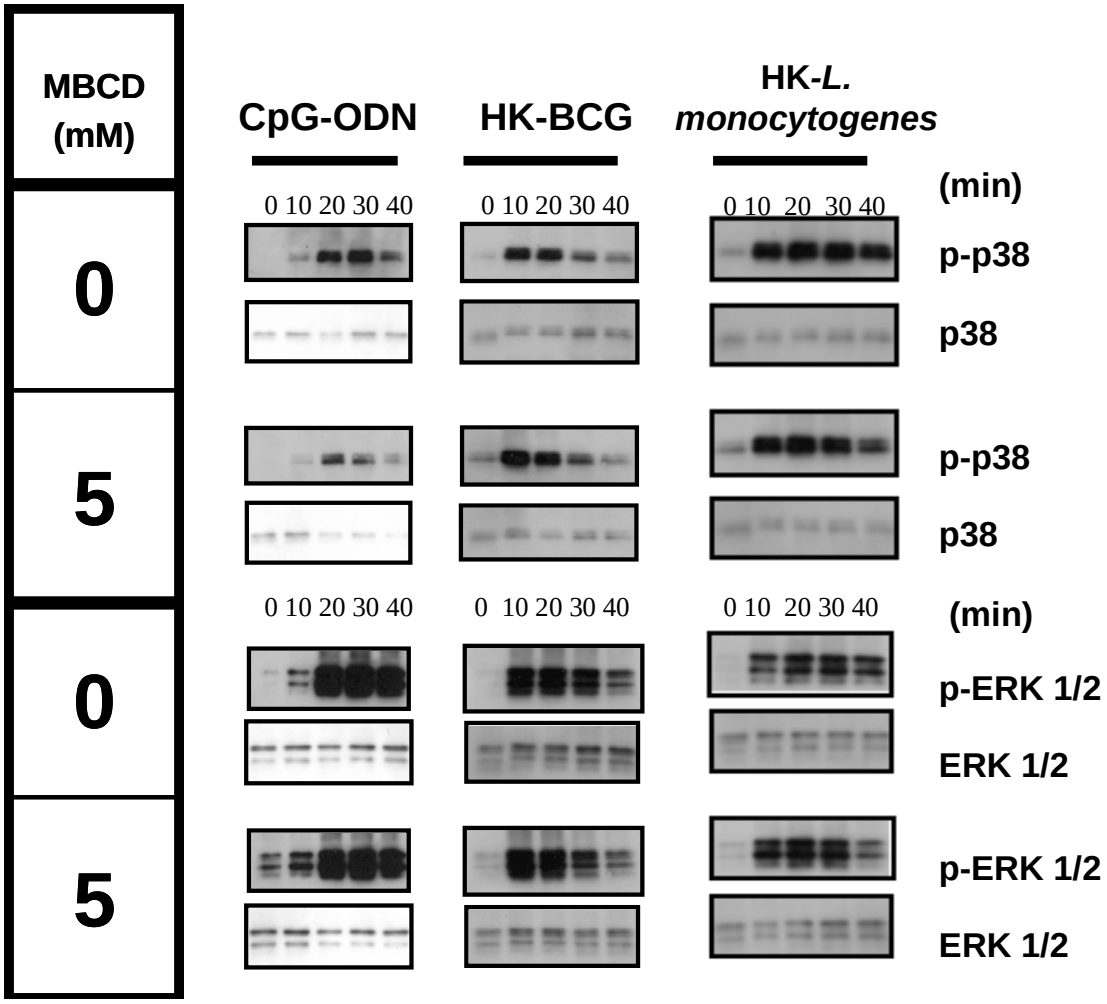
MBCD (mM)
0
5
0
5
CpG-ODN
HK-BCG
HK-L. monocytogenes
0 10 20 30 40
(min)
p-p38
p38
p-ERK 1/2
ERK 1/2

Fig. 5

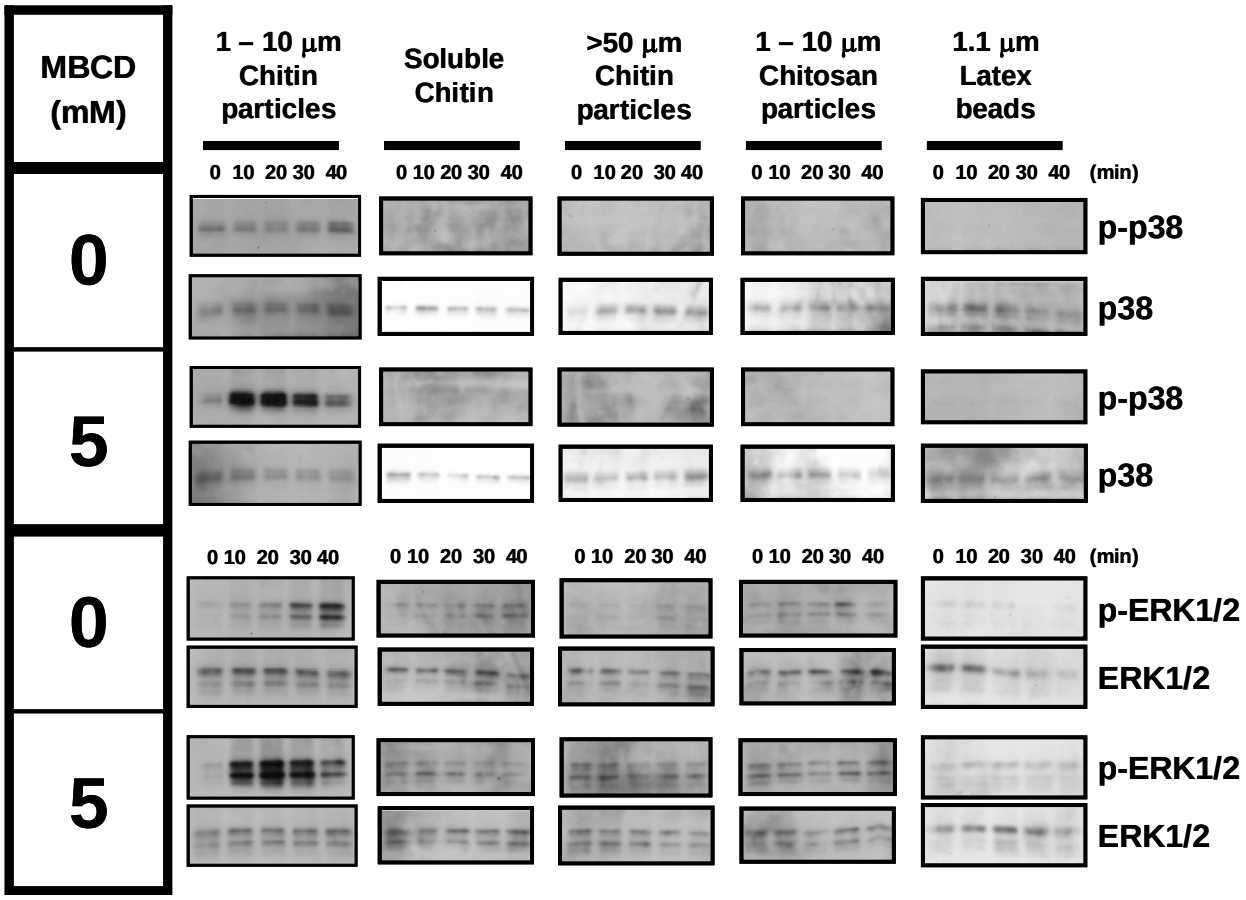
MBCD (mM)
1 – 10 μm Chitin particles
Soluble Chitin
>50 μm Chitin particles
1 – 10 μm Chitosan particles
1.1 μm Latex beads
0 10 20 30 40 (min)
0
5
p-p38
p38
p-ERK1/2
ERK1/2

Fig. 6

A)

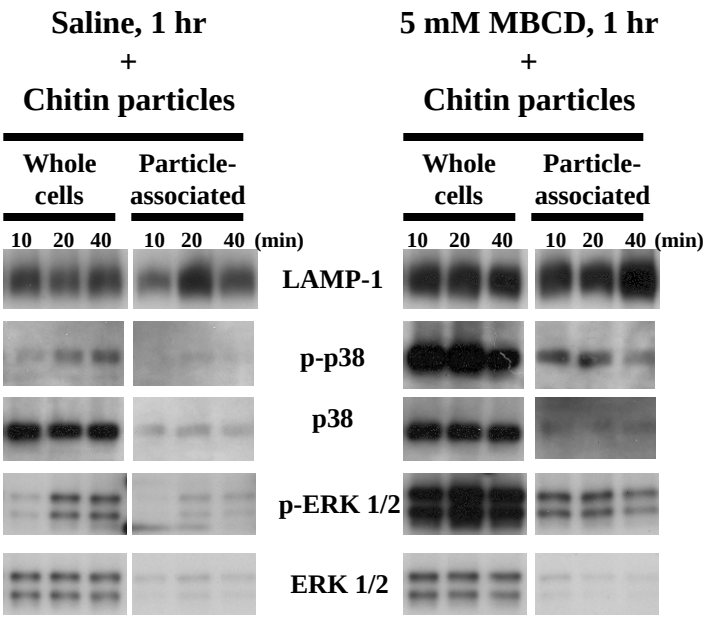
Saline, 1 hr
+
Chitin particles
5 mM MBCD, 1 hr
+
Chitin particles
Whole cells
Particle-associated
Whole cells
Particle-associated
10 20 40 10 20 40 (min)
10 20 40 10 20 40 (min)
LAMP-1
p-p38
p38
p-ERK 1/2
ERK 1/2

B)

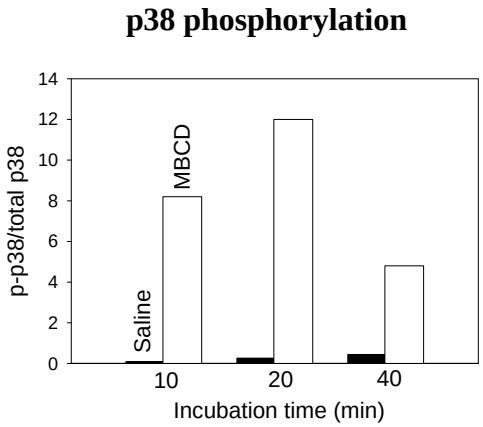
p38 phosphorylation
p-p38/total p38
Saline
MBCD
0
2
4
6
8
10
12
14
10
20
40
Incubation time (min)

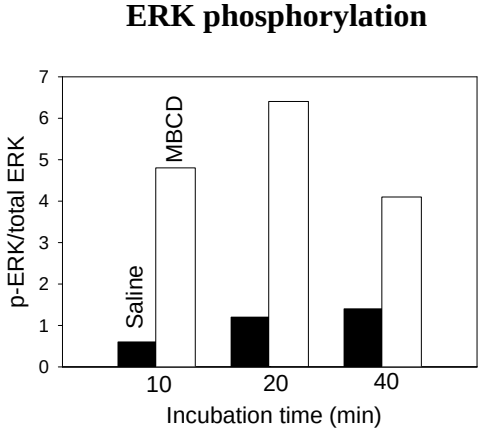
ERK phosphorylation
p-ERK/total ERK
Saline
MBCD
0
1
2
3
4
5
6
7
10
20
40
Incubation time (min)

Fig. 7

(A)

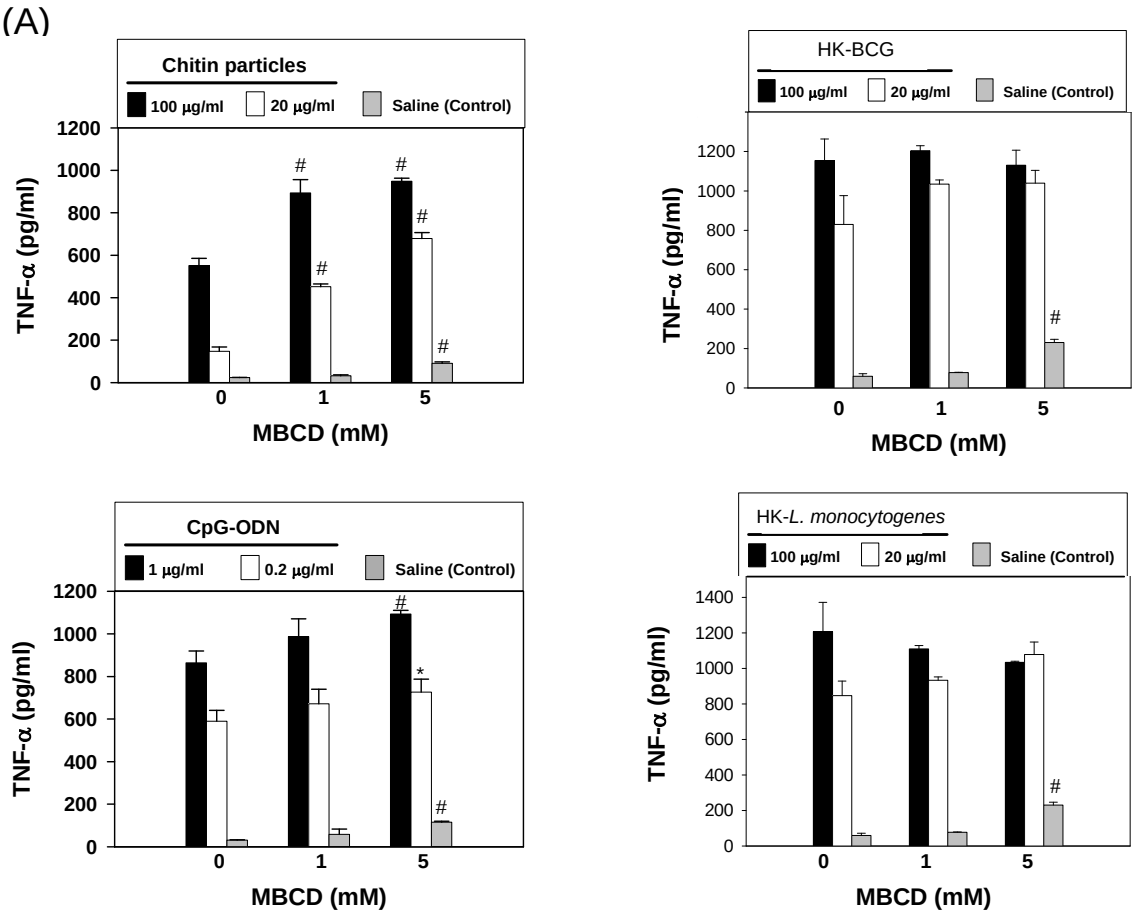
Chitin particles
100 μg/ml
20 μg/ml
Saline (Control)
TNF-α (pg/ml)
MBCD (mM)
HK-BCG
CpG-ODN
1 μg/ml
0.2 μg/ml
HK-L. monocytogenes

(B)

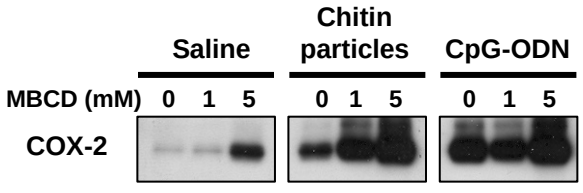
Saline
Chitin particles
CpG-ODN
MBCD (mM) 0 1 5 0 1 5 0 1 5
COX-2

(C)

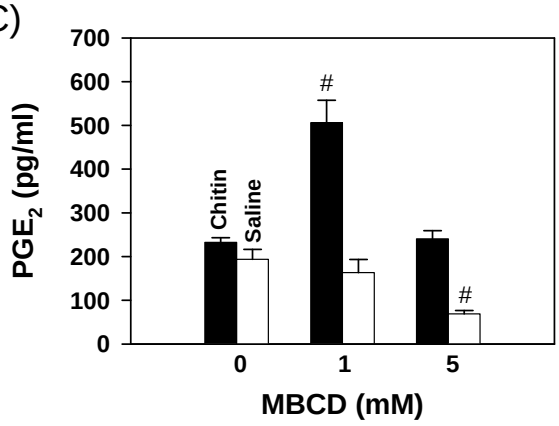
PGE2 (pg/ml)
Chitin
Saline
MBCD (mM)

Fig. 8